

Check for updates

# **Engineering Framework Materials in Water Systems for** Targeted Ion Extraction and Spontaneous Energy Harvesting

Zhengyun Wang, Miao Zhang,\* Hongfang Liu,\* and Wai-Yeung Wong\*

Developing techniques that can extract required salt resources and harvest spontaneous energy from natural water environment is essential to promote the global decarbonization and electrification. Construction of advanced framework materials with intrinsic nanochannels has been considered the most promising solution to implement this technique owing to the specific fluid transport performances in such confined space. However, this design requires a deep understanding of the structural properties of framework material nanochannels in different scenarios, as well as the corresponding construction strategies. Consequently, it is an urgent necessity to elucidate the specific ion capture behavior and fluid transport mechanism in these framework materials to build targeted nanofluidic systems for guiding developments in water related resources and energy acquisition technologies. Herein, the recent advances in ion extraction and energy harvesting based on metal-organic framework and covalent-organic framework materials have been outlined, along with the discussion about the nanochannels specificity by combining ions and fluid properties and nanochannel structures. Finally, an outlook to trends, challenges and emerging opportunities is given to foresee the future developments in this important field.

1. Introduction

Human civilization relies on water. Throughout history, human societies have greatly progressed by making full use of

Z. Wang, M. Zhang, W.-Y. Wong

Department of Applied Biology and Chemical Technology and Research Institute for Smart Energy

The Hong Kong Polytechnic University

Hung Hom, Hong Kong 999077, P. R. China

E-mail: bjtumiao.zhang@polyu.edu.hk; wai-yeung.wong@polyu.edu.hk

School of Chemistry and Chemical Engineering

State Key Laboratory of Materials Processing and Die & Mold Technology Key Laboratory of Material Chemistry for Energy Conversion and Storage (Ministry of Education)

Hubei Key Laboratory of Material Chemistry and Service Failure Huazhong University of Science and Technology (HUST) Wuhan 430074, P. R. China

E-mail: liuhf@hust.edu.cn

The ORCID identification number(s) for the author(s) of this article can be found under https://doi.org/10.1002/adma.202501881

© 2025 The Author(s). Advanced Materials published by Wiley-VCH GmbH. This is an open access article under the terms of the Creative Commons Attribution-NonCommercial-NoDerivs License, which permits use and distribution in any medium, provided the original work is properly cited, the use is non-commercial and no modifications or adaptations are made.

DOI: 10.1002/adma.202501881

natural water resources such as agricultural irrigation and industrial utilization.[1-3] Nowadays, the ever-increasing demand for matter and energy has motivated the research communities to seek and develop advanced techniques for gaining salt and electricity from water resources, which is essential to sustainable development of human society.[4-7] The lakes and sea contain huge water and various metal ions. In particular, specific ion extraction from these water sources such as lithium (Li), sodium (Na), uranium (U), and fluorine (F) not only provides solid matter foundation of modern battery industry and nuclear energy technology, but also significantly reduces the potential influences of poisonous ions on the environment and drastically improve public health.[8-12] Regarding the water based renewable energy harvesting, an important environmental factor is the constant salinity gradient between river water and seawater.[13] The

free energy for spontaneous mixing driven by osmotic pressure between these two types of water has been estimated to be 2.2 kJ per liter of freshwater and the total energy could reach 2 TW per year when regarding the flow rate of rivers to sea as the limiting factor.[14] This promotes the researchers to study the reverse electrodialysis method to harvest the substantial osmotic energy because of spontaneous rivers flow to seawater.[15-18] On the other hand, natural evaporation of water is also a reliable renewable energy resource,[19] and this process can generate electricity by converting the thermal energy of the air through electrokinetic effect.<sup>[20]</sup> Considering the giant reserve of water on the earth and continuous evaporation process, water evaporation induced electricity generation has been regarded as another promising blue energy conversion technique and has gained massive attention in the recent years.[21-25]

Toward targeted ion extraction and osmotic energy conversion, nanochannels play a critical role in ion recognition and selective transport. $[\hat{26}-30]$  In principle, when mixed ions flow through the specific nanochannels, the targeted ions could be efficiently transported through the nanochannels or directly be captured by nanochannels due to channel selectivity, while other ions would be rejected.[31,32] For the selective transport of ions in nanochannels driven by osmotic pressure between two different water phases, a net current would be generated and thus chemical potential energy is converted to electricity in this process.<sup>[33–35]</sup> In regard to water evaporation induced electricity generation,

15214095, 0, Downloaded from https://advanced.onlinelibrary.wiley.com/doi/10.1002/adma.202501881 by HONG KONG POL YTECHNIC UNIVERSITY HU NG HOM, Wiley Online Library on [2609/2025]. See the Terms

om/terms-and-conditions) on Wiley Online Library for rules of use; OA articles are governed by the applicable Creative Commons

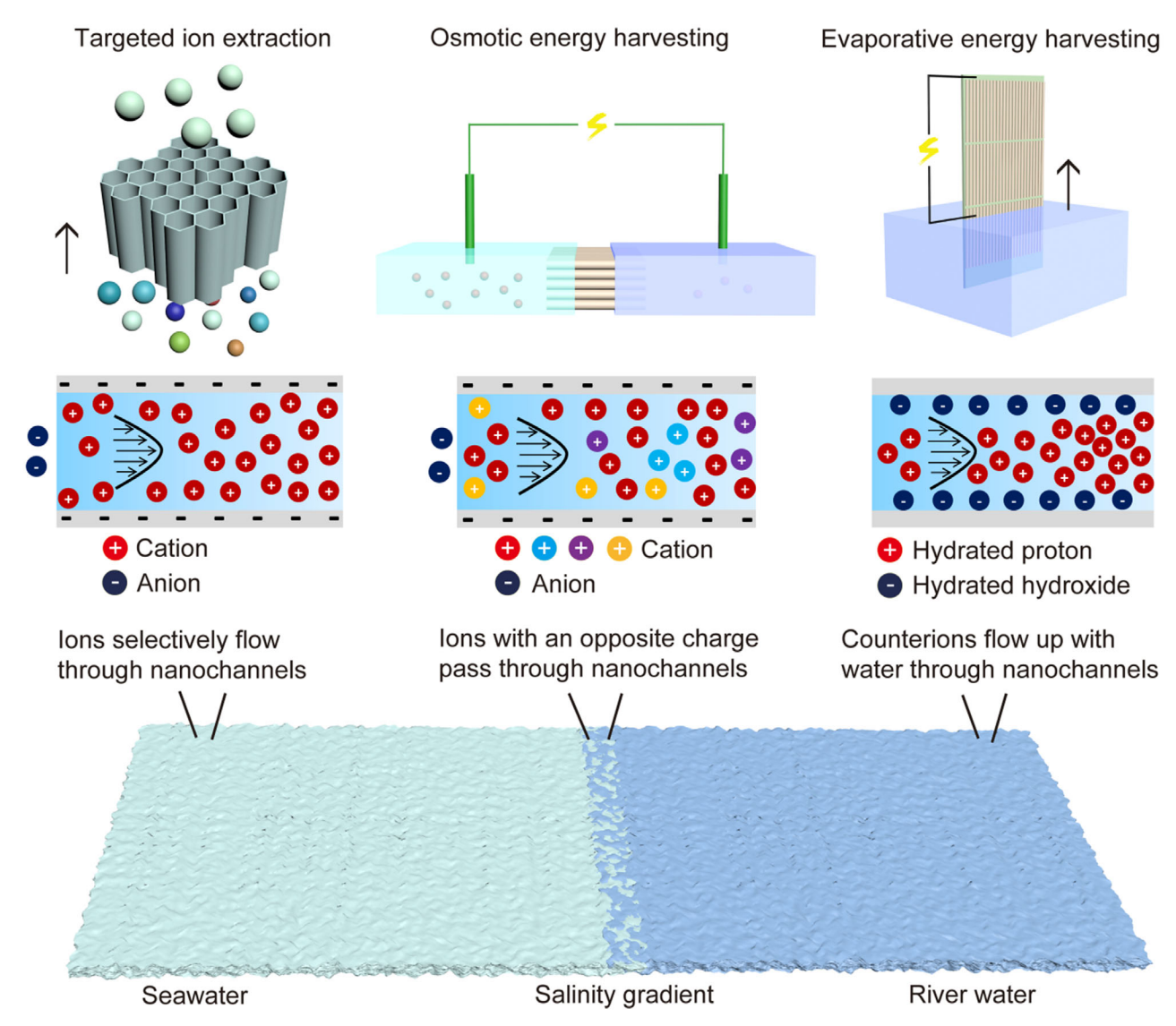


Figure 1. Water-based ion extraction, osmotic, and evaporative energy harvesting. Selective ion flow in nanochannels of framework materials plays a determining role in these applications.

nanochannels are also essential to water flow and ion transport. Specifically, the nanochannel walls are charged in water due to the formation of electrical double layer and the counterions with an opposite charge polarity would be pushed to another end with water flow driven by capillary force. [36–38] Water evaporation guarantees the continuity of capillary flow in nanochannels, and thereby a streaming potential is generated. [39] Comprehensively, nanofluidics is the pivotal foundation for the above water-matter and water-energy application, as displayed in Figure 1. Certainly, the requirements for nanochannel selectivity differ across these three applications. In ion extraction, the emphasis is on the purity of the targeted substance, necessitating higher ion selectivity of nanochannels. In contrast, osmotic and evaporation energy harvesting methods are primarily concerned with energy levels, namely charge separation, which results in a comparatively lower demand for selectivity. Particularly for electricity generation from water evaporation, the process relies more heavily on the migration of protons rather than other ions. Benefitting from the rapid development of membrane science and nanotechnology, in recent years, many nanofluidic devices based on 2D materials such as graphene, [40] graphite-mica, [41] MXene, [42,43] BN, [44] MoS<sub>2</sub>, [45,46] NbOPO<sub>4</sub>, [47] polymers, [48] and organic framework materials, [49,50] have been creatively fabricated to show impressive performances in ion sieving and energy harvesting. Among all these materials, framework materials including metalorganic frameworks (MOFs) and covalent-organic frameworks (COFs), are the most promising candidates for constructing hybrid nanofluidic systems owing to their well-defined porous structures, excellent ion selectivity, and good workability.[51,52] Structurally, MOFs and COFs are a family of crystalline porous framework materials based on organic linkers.<sup>[53]</sup> The difference between MOFs and COFs lies in the different patterns of connection, that is, coordination bonding of metal with organic linker and covalent bonding of organic unit are included in MOFs and COFs, respectively.<sup>[54]</sup> From the perspective of pursuit for high performances and wide applicability, the tremendous diversity





www.advmat.de

of MOF and COF families offer more possibilities to explore and customize the corresponding nanofluidic devices with required properties, including efficient separation of targeted ions and fast transport of water molecules in confined spaces. This is undoubtedly the most prominent advantage for framework materials in contrast to other materials. Notably, other emerging framework materials including hydrogen-bonded organic frameworks (HOFs), [55,56] porous aromatic frameworks (PAFs), [57] crystalline porous organic salts (CPOS),[58] and metal-graphdiyne frameworks (MGFs)[59] also inherently possess microporous architectures. However, apart from one report on HOFs for osmotic energy harvesting, [60] other framework materials have not yet been reported in the aforementioned technologies. Therefore, the framework materials currently applied in the nanofluidic fields are limited to MOFs and COFs, and performances of other framework materials in these technologies warrant further exploration in the future.

Systematic investigation of the designed strategies, fabrication methods and underlying mechanisms offers dual pathways for advancing nanofluidic technologies, refining established systems while pioneering innovative nanofluidic systems based on framework materials, ultimately enabling high performances and excellent practicality in ion-selective extraction and spontaneous energy harvesting. Nonetheless, establishing an accurate structure-activity relationship in correlated functions of these framework materials still poses a formidable challenge for the scientific communities. Based upon the current study on framework materials-related nanofluidics, this review examines the recent advances and breakthroughs in the design, fabrication, phenomenon and mechanism understanding of MOFs and COFs in the application of ion extraction and energy harvesting. Also, we discuss and emphasize the ion transport selectivity-related structural features of nanochannels in framework materials by combining chemical structures, geometry, orientation and interactions. We put forward the opportunities and critical challenges for the customization of future framework materials with desired function, with a particular focus on the deep study on nanofluidics and high throughput manufacturing methods. This review presents the first comprehensive analysis of framework materials in water-related applications, spanning ion extraction, osmotic energy conversion, and evaporative energy harvesting. The work not only establishes interdisciplinary synergies focusing on ion-selective transport mechanisms across these domains, but also identifies critical challenges and knowledge gaps in existing studies, providing valuable insights for future fundamental and applied research on water-related matter and energy.

## 2. Targeted Ion Capture and Extraction

## 2.1. MOFs for Ion Sieving

An ideal nanochannel for the extraction of targeted ions possesses an ultra-selective capability to allow monotypic ions transport. In this aspect, some natural biological ion channels with outstanding ion selectivity provide a highly efficient template for mimicking and constructing artificial ion channels.<sup>[61]</sup> This is usually a source of inspiration for researchers. But different from high bar for ion selectivity of natural ion channels, MOFs and

COFs based ion nanochannels also allow the transport of water molecules. Ion hydration always occurs in the presence of water, which would result in a highly complex process for ions access and transport in such confined channels because dehydrationrehydration is always involved. [62] For example, when permeating a narrow polymeric nanochannel with size smaller than that of solvated ions, the average hydration number of alkali-metal ions including Li+, Na+, and K+ is discovered to decrease and these ions cannot hold more than two water molecules.[63] Indeed, it needs to be acknowledged that although the energy barrier for transport of the various ions is different, realizing highly selective transport of ions in nanochannel of framework materials is not an easy task due to the highly close sizes for hydrated ions. [64] On the other hand, constructing bulky nanofluidic devices based on MOFs for the accurate measurement of sieving performances also adds an extra challenge because it is difficult to fabricate large area freestanding and robust MOF membranes.

The early method to explore ion-selective transport in MOFs is to use porous aluminum oxide as the substrate to support the MOF membranes, such as HKUST-1, ZIF-8, and UiO-66.[65,66] These deposited MOF membranes on porous aluminum oxide show different monovalent ion transport behavior. But in a strict sense, the nanochannels based on these pure MOFs have not been perfectly constructed because some other materials including graphene oxide nanosheets or polystyrene sulfonate were also incorporated in these MOF membranes. Therefore, the overall ion sieving performance is not entirely attributed to the MOFs. In order to first solve the problem of MOF nanochannels construction, in 2019, Wang and his collaborators proposed a representative way to construct nanochannels on the basis of MOFs.[11] Specifically, by using the ion track etching method, a 12 µm thick single bullet-shaped nanochannel was successfully embedded within a polyethylene terephthalate (PET) membrane. Taking this membrane as a support for MOF accommodation, the UiO-66-X MOF crystals (X represents H, NH<sub>2</sub>, and N<sup>+</sup>(CH<sub>3</sub>)<sub>3</sub>) were further in-situ grown in this nanochannel via a solvothermal reaction (Figure 2a). Then this channel was completely filled by UiO-66-X MOF crystals for ion transport. Interestingly, the current-voltage (I-V) measurement result shows that the UiO-66, UiO-66-NH<sub>2</sub>, and UiO-66-N<sup>+</sup>(CH<sub>3</sub>)<sub>3</sub> exhibit F<sup>-</sup> ion transport behavior (Figure 2b-d). The UiO-66-N<sup>+</sup>(CH<sub>3</sub>)<sub>3</sub> enables the highest selective F<sup>-</sup> ion transport over other anions including Cl<sup>-</sup>, Br<sup>-</sup>,  $I^-$ ,  $NO_3^-$  and  $SO_4^{2-}$  and the selectivity of  $F^-/Cl^-$  can reach 192 at a molar ratio of 1 (1.0 M KF/1.0 M KCl). Such high F- transport behavior is dominated by positive charge density on MOF crystals in water and the positive charge density can reach the highest vain UiO-66-N<sup>+</sup>(CH<sub>3</sub>)<sub>3</sub>. And the radial distribution function analysis from molecular dynamics simulations demonstrates a much weaker second hydration shell of F-, hinting a higher dehydration energy for F- ions to transport in small windows of UiO-66-N<sup>+</sup>(CH<sub>3</sub>)<sub>3</sub>. This work first realizes the selective F<sup>-</sup> transport based on MOFs and also establishes the nanofluidic construction method for precisely evaluating ion-selective transport behavior in MOF crystals. Following this research work, some similar devices have been fabricated based on other MOFs such as UiO-66-COOH and MIL-53-COOH for selective transport of monovalent metal ions including K<sup>+</sup>, Na<sup>+</sup> and Li<sup>+</sup>. [49,67,68] But the multivalent metal ions (Ca2+ and Mg2+) have been discovered to be unable to pass through the channels of these MOFs under the

wiley.com/doi/10.1002/adma.202501881 by HONG KONG POLYTECHNIC UNIVERSITY HU NG HOM, Wiley Online Library on [26/09/2025]. See the Term

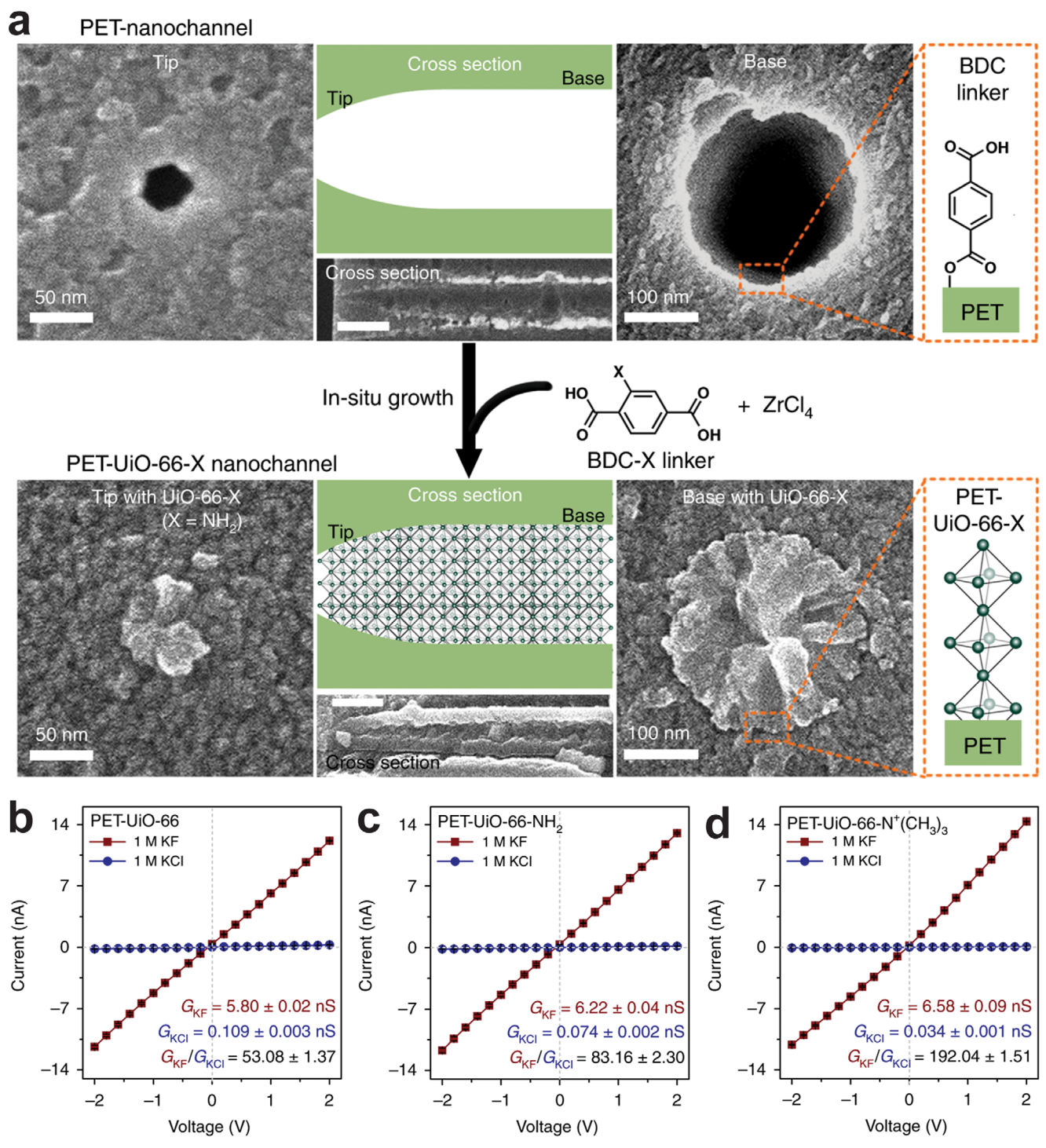


Figure 2. PET-housed MOF as the F- channel. a) Scanning electron microscope figures of PET-nanochannels before and after filling MOF UiO-66-X. I-V measurement of b) PET-UiO-66, c) PET-UiO-66-NH<sub>2</sub>, and d) PET-UiO-66-N<sup>+</sup> (CH<sub>3</sub>)<sub>3</sub> in KCl and KF. a-d) Reproduced under the terms of the CC-BY Creative Commons Attribution 4.0 International license. [11] Copyright 2019, X. Li et al., published by Springer Nature.

external electric field. This phenomenon can be attributed to the hindrance caused by the stronger Coulomb forces.

After these works, many MOF-ion sieving related researches based on electrodialysis have been continuously reported. So far, the UiO-66 MOF and its derived MOF have gained sufficient popularity in ion sieving. The fundamental reason lies in tunable chemical structure in channels and excellent water stability of UiO-66. Essentially, spatial structure, charged density and constructional porosity of MOFs determine the ion-selective transport property.[69-72] Continuing with UiO-66 as an example, the





www.advmat.de

pore window size of UiO-66 is ≈6.0 Å. Introduction of polar chemical groups or molecules into benzene ring of the UiO-66 linker is a universal strategy to realize screening of monovalent ions, as this not only further reduces the size of the channel window but also directly alters the charged behavior of channel in water. For instance, some groups including -NH<sub>2</sub>, -SH, -OH, and -OCH, have been selected to functionalize UiO-66 and the results show that K<sup>+</sup>/Mg<sup>2+</sup> selectivity of the UiO-66-(OCH<sub>3</sub>)<sub>2</sub>, UiO-66-(OH)<sub>2</sub>, UiO-66-(SH)<sub>2</sub> and UiO-66-(NH<sub>2</sub>)<sub>2</sub> with a test area of 3.14 mm<sup>2</sup> are 1567.8, 542.9, 92.0, and 4.9 at a molar ratio of 1 (0.5 M chlorate salts), respectively.<sup>[73]</sup> In the same way, the introduction of molecules, such as crown ether introduction into UiO-66 also brings similar effects on monovalent ion transport. Such transport behavior difference should be highly correlated with the different ion affinity of functional groups or molecules. A more important breakthrough lies in the realization of sodium-selective subnanochannels in MOFs. Subnanoconfinement of 4'-aminobenzo-15-crown-5 ether into UiO-66 would lead to preferential transport of Na<sup>+</sup> over K<sup>+</sup> and Li<sup>+</sup>, as shown in Figure 3a.[74] Such functionalized UiO-66 (15-C5-MOF) can serve as an effective artificial Na+-selective subnanochannel. The Na<sup>+</sup>/K<sup>+</sup> and Na<sup>+</sup>/Li<sup>+</sup> selectivity can be up to 360.1 and 1770.0 at a molar ratio of 1 (1 M chlorate salts), respectively (Figure 3b), and these selectivity values are comparable to the high selectivity of biological sodium channels. The authors attributed the high Na selectivity to size, charge, hydrophobicity and binding capability of 4'-aminobenzo-15-crown-5 ether functionalized UiO-66 channels.

Given the selective monovalent ion sieving properties exhibited by MOFs, the researchers have directed their attention to the Li<sup>+</sup> ion extraction from salt-lake brines and other water resources because Li is a significant metal widely used in batteries.<sup>[75]</sup> In this aspect, Li<sup>+</sup>/Mg<sup>2+</sup> selectivity is an important performance index owing to the presence of Mg<sup>2+</sup> ions as co-existing interference in large quantities. Some MOFs with good Li<sup>+</sup>/Mg<sup>2+</sup> selectivity include UiO-67,[76] UiO-66-(COONa)2,[77] UiO-66-(SH)2,[78] UiO-66-NH<sub>2</sub>/ZIF-8,<sup>[79]</sup> and ZIF-7 encapsulated with benzo-12crown-4-ether.[80] Among these MOFs, the UiO-66-(SH), MOF demonstrates the highest Li<sup>+</sup>/Mg<sup>2+</sup> selectivity. In a PET substrate with small pores (pore size of 29.7  $\pm$  6.0 nm, pore density of  $10^6$  cm<sup>-2</sup>), the UiO-66-(SH), crystals with window size of 4.7 Å, and cavity sizes of 8 and 11.7 Å shows Li<sup>+</sup>/Mg<sup>2+</sup> selectivity of 1516 under 0.2 molar ratio of Mg<sup>2+</sup>/Li<sup>+</sup> (0.1 M chlorate salts) for the feed solution (Figure 3c,d). And the Li<sup>+</sup>/Mg<sup>2+</sup> selectivity is still capable of reaching 19 when the mole ratio of Mg<sup>2+</sup>/Li<sup>+</sup> increases to 30 (Figure 3e), manifesting the purity of lithium products can reach a high level (95.0-99.9%). Another recent research advance involves a sustainable regeneration design in MOFs. Wu et al. proposed a sunlight-regenerable strategy, that is, confining polyspiropyran (PSP) into UiO-66 to achieve PSP-UiO-66 because spiropyran is a sunlight-responsive molecule that can act as Li<sup>+</sup> adsorption sites.[81] In dark conditions, spiropyran can transform to zwitterionic species with the capability to adsorb cations and anions. While in visible light conditions, it would reverse back and release the adsorbed ions. The UiO-66 with spiropyran shows a Li<sup>+</sup>/Mg<sup>2+</sup> selectivity of 29.49 and 5.83 in synthetic brines with Mg/Li ratios of 0.1 and 1, respectively, and a high adsorption capacity of 10.17 mmol g<sup>-1</sup> in dark conditions. More importantly, UiO-66 has exhibited rapidly regeneration performances under sunlight irradiation, suggesting a fast adsorption-desorption process in salt solutions. This work did not adopt the commonly used electrochemical method in nanofluidics, but instead of light energy to supply power, providing important inspiration for sunlight based ion extraction. As for other important ion extraction based on MOFs, such as uranium (U) and lead (Pb), [82,83] the key to achieve high capture performance is also to confine groups or molecules with high affinity for target ions in the MOF channels. The difference is making these ions to be directly adsorbed inside the MOF channels. For example, UiO-66 and its NH<sub>2</sub> based derivatives show uranium adsorption capacity in water. [84]

Overall, the ion selectivity is significantly affected by polar functional groups of the subnanochannels in MOFs. Taking Li ion extraction as an example, current works focus on UiO-66 and modulation of Li<sup>+</sup>/Mg<sup>+</sup> selectivity by introduction of polar groups into the ligand. Nevertheless, some other MOFs with excellent water stability have been completely ignored, such as STAM-17-OEt.<sup>[85]</sup> Some molecules have been introduced into the UiO-66 nanochannels to offer a confined effect or to change charged density, for targeted ion selective transport, but specific location, structure and loading density of these guest molecules in MOF nanochannels is still unknown. The whole framework structures have not been precisely characterized although the modified MOFs show reduced pore size and specific area by Brunauer-Emmett-Teller analysis. In terms of structure, the Ångström-scale pore sizes, cavities and configurations of MOFs also greatly influence the ion transport. A typical example is that cations display lower mobility in UiO-66 than MIL-53 and Al-TCPP (Figure 3f).[69] This phenomenon may be related to the high complexity degree of the 3D channels in UiO-66. On the contrary, UiO-66 has octahedral and tetrahedral cavity, as well as triangular window while MIL-53 and Al-TCPP only have 1D and 2D channels, respectively (Figure 3g). These facts indicate that there is still a significant room for improvement of ion selectivity in MOF channels. On the other hand, the influence of other substances including K<sup>+</sup> and Na<sup>+</sup> ions cannot be overlooked in Mg-Li separation because these interfering substances still exist in actual industrial conditions.

Also, the whole ions flux is at a low level for a single nanochannel housed MOFs in the PET membrane, indicating a low yield for targeted ions. Meanwhile, the understanding of ionic transport behavior in PET nanochannel housed MOFs is still relatively superficial. The rectification effect, ion current saturation, and ohmic behavior frequently occur in PET nanochannel housed MOFs and most studies attribute the selectivity solely to the sieving action of MOF micropores. However, these ionic transport behaviors cannot be fully explained from the perspective of micropores alone. Studies of Omar Azzaroni and Matías Rafti have revealed the important role of constructional porosity in transport properties within such confined spaces.<sup>[70,86,87]</sup> In their works, employing different growth methods to accommodate UiO-66 in PET nanochannel would result in diverse constructional porosity, which strongly influences the rectification behavior and ion current saturation. Due to the dependence of the charge state of UiO-66 on the degree of protonation, changes in pH can enable the switching of iontronic output among different regimes. These findings imply that different growth methods lead to heterogeneous structures and asymmetric distributions of MOFs within the nanochannels. Such constructional porosity may also



15214095, 0, Downloaded from https://advanced.onlinelibrary.wiley.com/doi/10.1002/adma.202501881 by HONG KONG POL YTECHNIC UNIVERSITY HU NG HOM, Wiley Online Library on [26/09/2025]. See the Terms

conditions) on Wiley Online Library for rules of use; OA articles are governed by the applicable Creative Commons

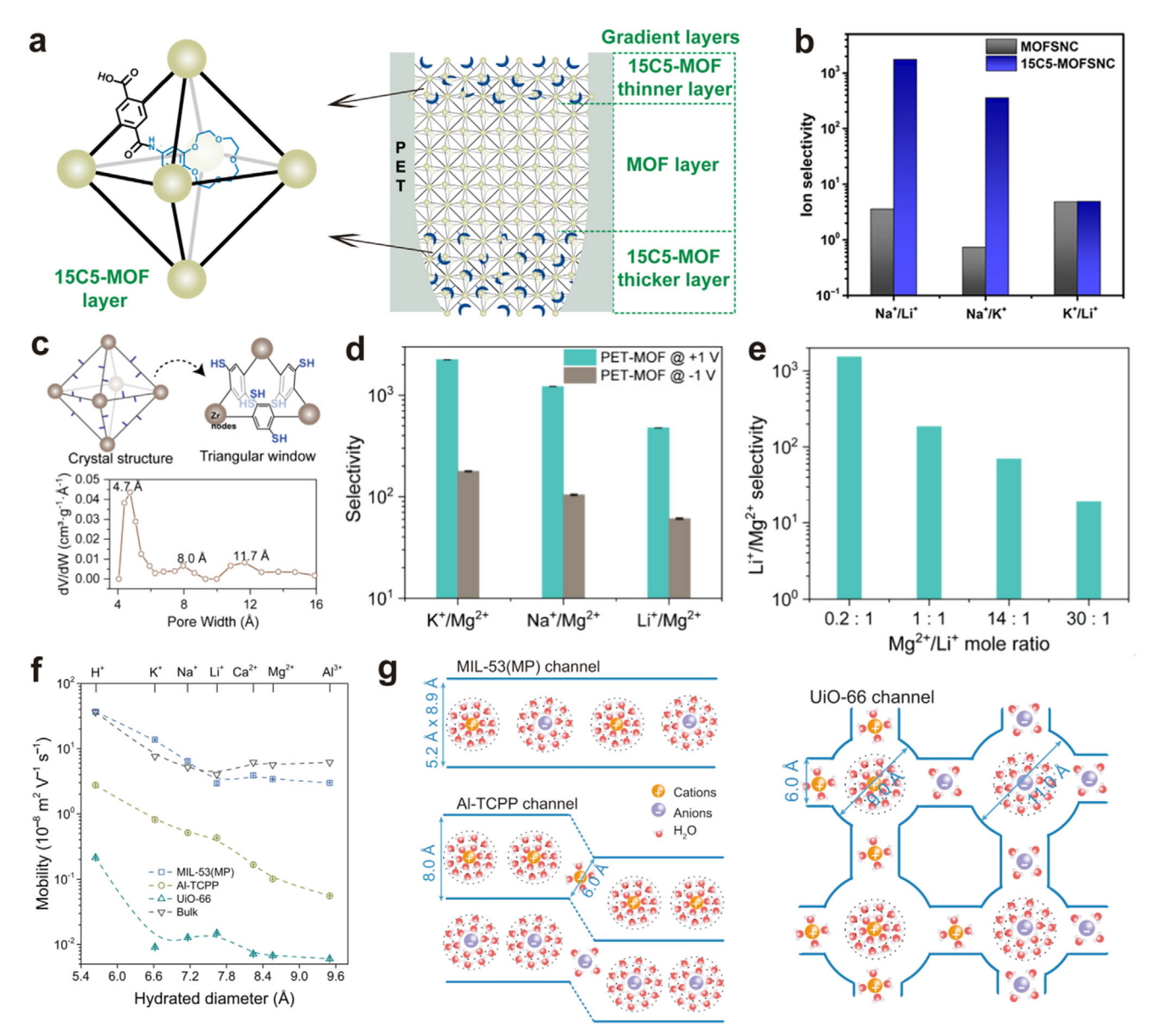
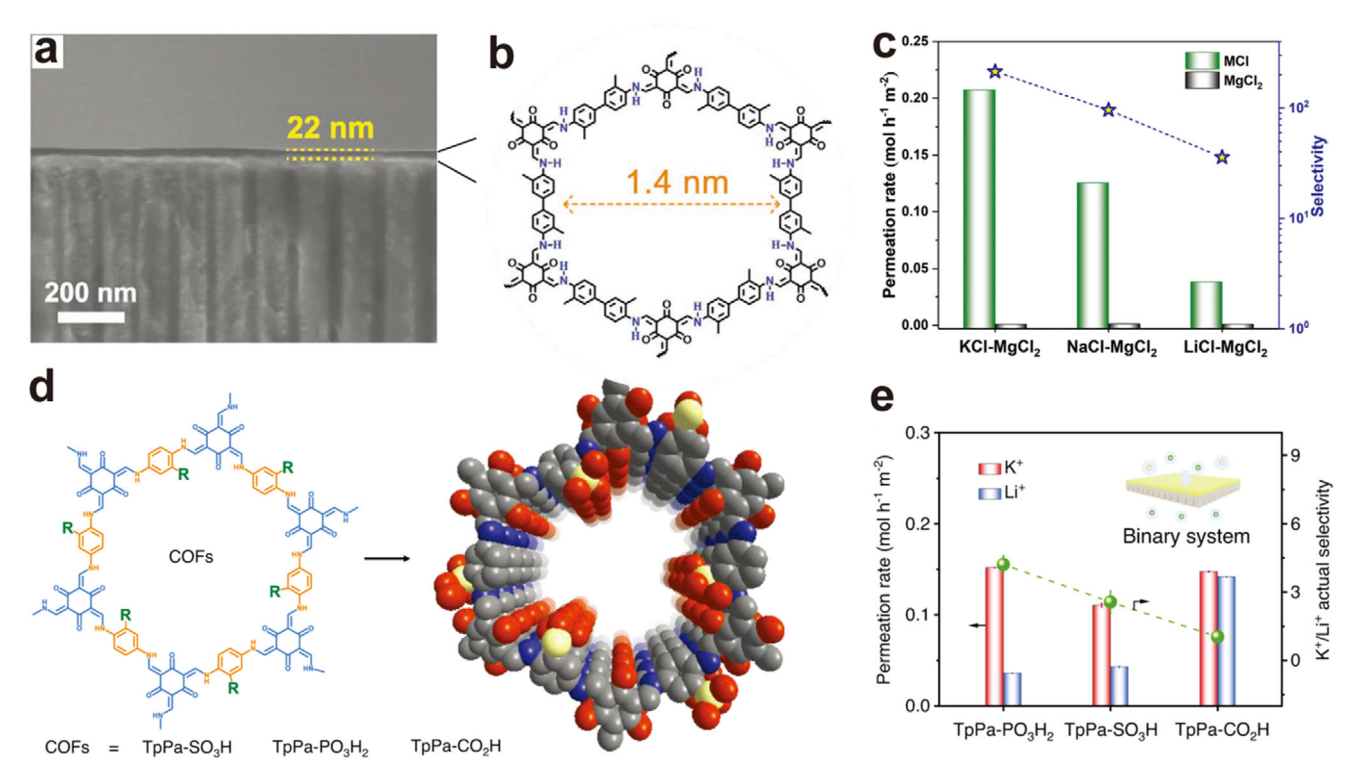


Figure 3. MOF structures and the corresponding ion-selective transport behavior. a) Subnanoconfinement of 4'-aminobenzo-15-crown-5 ether into UiO-66 to achieve 15-C5-MOF layer and filling PET nanochannel with this MOF as the gradient layers. The whole PET-MOF can serve as an artificial selective Na+ channel. b) Monovalent ion selectivity comparison between UiO-66 and 15-C5-MOF. a,b) Reproduced with permission. [74] Copyright 2023, American Association for the Advancement of Science. c) Crystal structure of UiO-66-(SH)2 and pore size analysis. d) K+/Mg<sup>2+</sup>, Na<sup>+</sup>/Mg<sup>2+</sup>, Li+/Mg<sup>2+</sup>, selectivity of PET-UiO-66-(SH), nanochannels. e) Li+/Mg<sup>2+</sup> selectivity of PET-UiO-66-(SH), nanochannels under different Mg<sup>2+</sup>/Li+ mole ratio. c-e) Reproduced with permission. [78] Copyright 2024, American Chemical Society. f) Mobility of different ions in MIL-53, Al-TCPP, UiO-66 nanochannels and bulk solution condition. g) Different channels structures of MIL-53, Al-TCPP, UiO-66. UiO-66 shows more complicated nanochannels than MIL-53 and Al-TCPP. f,g) Reproduced under the terms of the CC-BY Creative Commons Attribution 4.0 International license. [69] Copyright 2023, X. Li et al., published by Springer Nature.

affect the ion selectivity, as the total charge of the multiple ion pathways provided by the constructional porosity may change to some extent. If attempts are considered to be taken to construct large area nanochannels in a membrane, this is feasible in terms of methodology while large-scale filling MOF crystals in the range of square meters in these etched nanochannels to ensure fairly consistent uniformity is currently unrealistic. Using counter-diffusion and one-pot interfacial growth methods may both result in the formation of constructional porosity during large-area filling. On the other hand, the form of MOFs in the artificial nanochannel in the PET membrane is polycrystalline, which means the nanochannels of MOFs are not in long-range ordered pattern. Such disorder MOF crystals filling poses a challenge for macroscopic modeling in the macro simulation of ion migration under electrical field, which could help us understand the flow behavior of a large number of ions.

15214095, 0, Downloaded from https://advanced.onlinelibrary.wiley.com/doi/10.1002/adma.202501881 by HONG KONG POLYTECHNIC UNIVERSITY HU NG HOM, Wiley Online Library on [2609)2025]. See the Terms and Conditions (https://onlinelibrary.wiley

and-conditions) on Wiley Online Library for rules of use; OA articles are governed by the applicable Creative Commons



**Figure 4.** COF structures and corresponding ion-selective transport behavior. a,b) Scanning electron microscope image of TpBDMe2 COF layer on AAO surface. The channel size is around 1.4 nm. c) Permeation rate and selectivity of TpBDMe2 COF/AAO in binary ion solution systems. a–c) Reproduced with permission. <sup>[50]</sup> Copyright 2021, Wiley. d) Introducing different chemical groups in TpPA COF to achieve TpPa-SO<sub>3</sub>H, TpPa-PO<sub>3</sub>H<sub>2</sub>, and TpPa-CO<sub>2</sub>H, respectively. The nanochannels in these COFs are 1D. e) Permeation rate and K<sup>+</sup>/Li<sup>+</sup> selectivity of TpPa-SO<sub>3</sub>H, TpPa-PO<sub>3</sub>H<sub>2</sub> and TpPa-CO<sub>2</sub>H COF membranes. d,e) Reproduced under the terms of the CC-BY Creative Commons Attribution 4.0 International license. <sup>[90]</sup> Copyright 2022, H. Wang et al., published by Springer Nature.

#### 2.2. COFs for Ion Sieving

Under normal circumstances, COFs always display 2D topological structures because the organic monomers are connected in a plane by strong covalent bonds, thereby most COFs exhibit the form of a membrane on a macroscopic level.[88] This property facilitates the construction of COFs based nanofluidic devices for ion sieving because it allows for the direct growth of COF films on the porous substrate surface. In 2021, Bing et al. first studied the Li extraction with COF membranes.<sup>[89]</sup> A series of COF membranes were constructed by using 1,3,5-tris(4-aminophenyl)benzene (TAB), 2,5-bis(2-(2-(2methoxyethoxy)ethoxy)terephthalaldehyde (4EO), as well as 2,5-bis(heptyloxy)terephthalaldehyde (OHep) as monomers. The COF-4EO and COF-OHep were grown on polyacrylonitrile (PAN) ultrafiltration membranes for the measurement of performances. Two completely different trends of ion transport selectivity have been exhibited, namely, an order of  $K^+$  $Na^{+} > Li^{+} > Mg^{2+} > Ca^{2+}$  and  $Li^{+} > K^{+} > Na^{+} > Ca^{2+} >$ Mg<sup>2+</sup> for COF-OHep and COF-4EO, respectively. With a test area of 3.14 cm<sup>2</sup>, the COF-OHep can afford a Li<sup>+</sup>/Mg<sup>2+</sup> separation factor of 12 but COF-4EO just shows a low selectivity of 3 at a molar ratio of 1 (0.1 M chlorate salts). In the same year, Xu's group also explored the selective ion sieving performances by using a COFs based membrane.<sup>[50]</sup> In their work, a thin COF membrane with 22 nm thickness was synthesized by using 1,3,5-triformylphloroglucinol (Tp) and 2,6-dimethylbenzidine (BDMe $_2$ ) as monomers (**Figure 4a**,b). The resultant TpBDMe $_2$  COF membranes with 1D nanochannels (1.4 nm) could form on the anodic aluminum oxide (AAO) surface. As expected, the monovalent ions (K $^+$ , Na $^+$ , Li $^+$ ) permeation rates for such device are much higher than those of the divalent and trivalent ions (Ca $^{2+}$ , Cu $^{2+}$ , Mg $^{2+}$ , Ni $^{2+}$ , La $^{3+}$ , Ce $^{3+}$ ). With a test area of 3.14 cm $^2$ , ion selectivity for K $^+$ /Mg $^{2+}$ , Na $^+$ /Mg $^{2+}$ , Li $^+$ /Mg $^{2+}$  is 765, 680, and 217 at a molar ratio of 1 (0.1 M chlorate salts), respectively (Figure 4c). The authors ascribe the ion selectivity to different electrostatic attraction generated by -NH groups toward cations.

After these two works, study on separation of monovalent cations based upon COF membranes began to emerge. A representative work is to use diamine monomer with different acid groups, including 2,5-diaminophenylphosphonic acid group (Pa-PO<sub>3</sub>H<sub>2</sub>), 2,5-diaminobenzenesulfonic acid group (Pa-SO<sub>3</sub>H), and 2,5-diaminobenzoic acid group (Pa-CO<sub>2</sub>H) that can react with Tp for exploring the separation of monovalent cations. [90] By using the porous polytetrafluoroethylene (PTFE) with an average pore size of 200 nm to support COFs, three kinds of COF membranes with pristine channels of 13 Å form on surface and PO<sub>3</sub>H<sub>2</sub>, SO<sub>3</sub>H, and CO<sub>2</sub>H are respectively contained in the nanochannel walls (Figure 4d). With mixtures of KCl and LiCl (0.1 M) as feed solution, the K<sup>+</sup>/Li<sup>+</sup> selectivity of TpPa-PO<sub>3</sub>H<sub>2</sub> and TpPa-SO<sub>3</sub>H membrane (1.54 cm<sup>2</sup>) are 4.21  $\pm$  0.37 and 2.56  $\pm$  0.49,



ADVANCED MATERIALS

www.advmat.de

respectively, but TpPa-CO<sub>2</sub>H membrane exhibits a lower K<sup>+</sup>/Li<sup>+</sup> selectivity of  $1.04 \pm 0.16$  (Figure 4e). The ion selectivity in such COFs is attributed to the different capabilities of acid groups to bind water molecules, which has been further revealed by characterizing the confined water layers via atomic force microscope and dielectric spectra. Another attractive physical phenomenon is to achieve switchable Na+ and K+ transport selectivity in a COF membrane.<sup>[91]</sup> The specific method is introducing the cysteine into a COF connected by 1,3,5-tris(4-aminophenyl)-benzene (TAPB), 2,5-dimethoxyterephthalaldehyde (PDA-OMe) and 2,5divinylterephthalaldehyde (PDA-V). It has been discovered that the cysteine functionalized COF (COF-Cys) membrane with 0.5 cm<sup>2</sup> is pH-responsive and can switch from K<sup>+</sup>-selective (K<sup>+</sup>/Na<sup>+</sup> selectivity of 1.7) to Na+-selective (Na+/K+ selectivity of 2.7) under a pH stimulus from 3.8 to 8.9 at a molar ratio of 1 (0.1 M chlorate salts). This switchable Na+/K+ selectivity is determined by coordination interactions between target ions and cysteine in the COF membrane.

At present, the research interests on the ion sieving and extraction with COFs are also starting to shift toward the lithium ion collection, such as using imine-linked 3D COF membranes with charged sub-1 nm channels to realize Li<sup>+</sup>/Mg<sup>2+</sup> separation.<sup>[92]</sup> A recent study on 3D COFs demonstrates the important role of counterion-mediated positively charged channels in efficient Li+ transport and such COF (COF-300-CH<sub>0.6</sub>) shows a high Li<sup>+</sup>/Mg<sup>2+</sup> selectivity of 321 in electrodialysis tests.<sup>[93]</sup> But overall, the corresponding research is still in the initial stages. Despite the fact that most of the current research on COF membranesrelated ion extraction is much less compared to that of MOFs, the adopted regulatory strategies for improving ion selectivity are generally basically identical, including introduction of organic chains or polar groups to change the charged effect, [94] and pore size[95] of pristine COFs. Most of these groups contain oxygen atoms that would tend to interact with confined water molecules and induce water ionization, resulting in negative charged wall of channels. This is favorable for selective transport of cations. Although these COF membranes exhibit some interesting ion-selective transport behavior such as pH stimulated selectivity switch, it should be acknowledged that the ion sieving performances of COF membranes have not reached the level of MOF materials except for Li+ ion sieving, which may be due to the larger pore size of COFs. On the other hand, it needs to be noted that some COF membranes such as TpPa-SO<sub>3</sub>H also demonstrate excellent salt rejection property, [96,97] that is, none of the ions can transport through nanochannels of COF membranes. The opposite experimental observations, namely, selective ion transport and excellent salt rejection properties of the COF membranes highlight a significant knowledge gap in fully understanding the characteristics of COF nanochannels. Similar to MOFs, there is a vast room for regulation of COF nanochannels for selective ion transport. Regarding the synthesis of large scale COF membranes on desired porous substrate, recent reports have introduced the scraping-assisted interfacial polymerization technique for fabricating scalable and uniform COFs.[98] This industrially adaptable method may show more advantages than traditional interfacial polymerization method and also provides a methodological foundation for exploring the ion extraction performances of more larger-area COF membranes.

Currently, lithium extraction from salt lakes stands as the most prominent industrial application for the selective extraction of targeted ions. To understand the actual performance gaps, it is essential to compare the performance of MOF- and COF-based systems with existing industrial membranes using methods of nanofiltration and electrodialysis. In the industrial Li+/Mg2+ separation via nanofiltration (NF), commercial membranes like polyamide (DK-1812 and NF90) typically show a relatively lower Li+/Mg2+ selectivity, ranging from 2 to 4.[99,100] Commercial cation and anion exchange membranes (CSO and ASA) demonstrate a Li+/Mg2+ selectivity ranging from 10 to 20 when the Mg<sup>2+</sup>/Li<sup>+</sup> ratio exceeds 5 during electrodialysis.[101] In contrast, the framework material-based membranes enable precise Mg-Li separation and show high Li<sup>+</sup>/Mg<sup>2+</sup> selectivity which surpasses that of the commercial membranes. Moreover, framework material-based membranes possess the potential for synergistic integration with an external field, such as solar-driven separation, which is a capability that is absent in commercial membranes. However, framework material-based membranes fall considerably short in engineering service life. Under actual operating conditions, commercial membranes can last for several months or even years, whereas framework material-based membranes have a maximum lifespan of only one month. In addition, the size of the membranes based on framework materials is smaller than that of the commercial membranes. Commercial membranes used for lithium extraction can reach sizes of hundreds of square centimeters,[102] while membranes based on framework materials are limited to a few or a dozen square centimeters. Hence, maintaining high ion selectivity and further enhancing the effective area, mechanical, and chemical stability of framework materials is a crucial focus at present, with the goal of achieving comprehensive performance comparable to industrial-grade standards.

### 3. Osmotic Energy Harvesting

### 3.1. MOFs for Osmotic Energy Harvesting

The research on MOFs in osmotic power harvesting could be traced back to the year of 2018. Some MOFs such as MOF-199 and Cu-TCPP were explored but showed relatively low energy conversion performances.[103,104] These studies have prompted the researchers to develop other MOF materials with high performances in osmotic energy conversion. In 2021, motivated by high ion-selective transport capability of UiO-66 and its derivatives, UiO-66-NH2 based osmotic energy generator with high performances was reported.[105] The UiO-66-NH2 layer supported by porous alumina is anion selective and its diffusion current density and voltage increase with higher KCl concentration gradient (Figure 5a,b). And the maximum output power densities are 4.93 and 2.96 W m<sup>-2</sup> under 50-fold KCl and NaCl gradients with an effective testing area of 0.03 mm<sup>2</sup>, respectively (Figure 5c). The authors ascribed the performance difference to the different hydrated diameter of Na+ ions and K+ ions. However, applying MOF particles in osmotic energy harvesting is meaningful but also difficult. About this issue, Xiao et al. gave a representative example.[106] In their approach, poly(methyl methacrylateco-vinylimidazole) was used to modify UiO-66-NH2 nanopar-

15214095, 0, Downloaded from https://advanced.onlinelibrary.wiley.com/doi/10.1002/adma.202501881 by HONG KONG POLYTECHNIC UNIVERSITY HU NG HOM, Wiley Online Library on [26/09/2025]. See the Terms

and-conditions) on Wiley Online Library for rules of use; OA articles are governed by the applicable Creative Commons

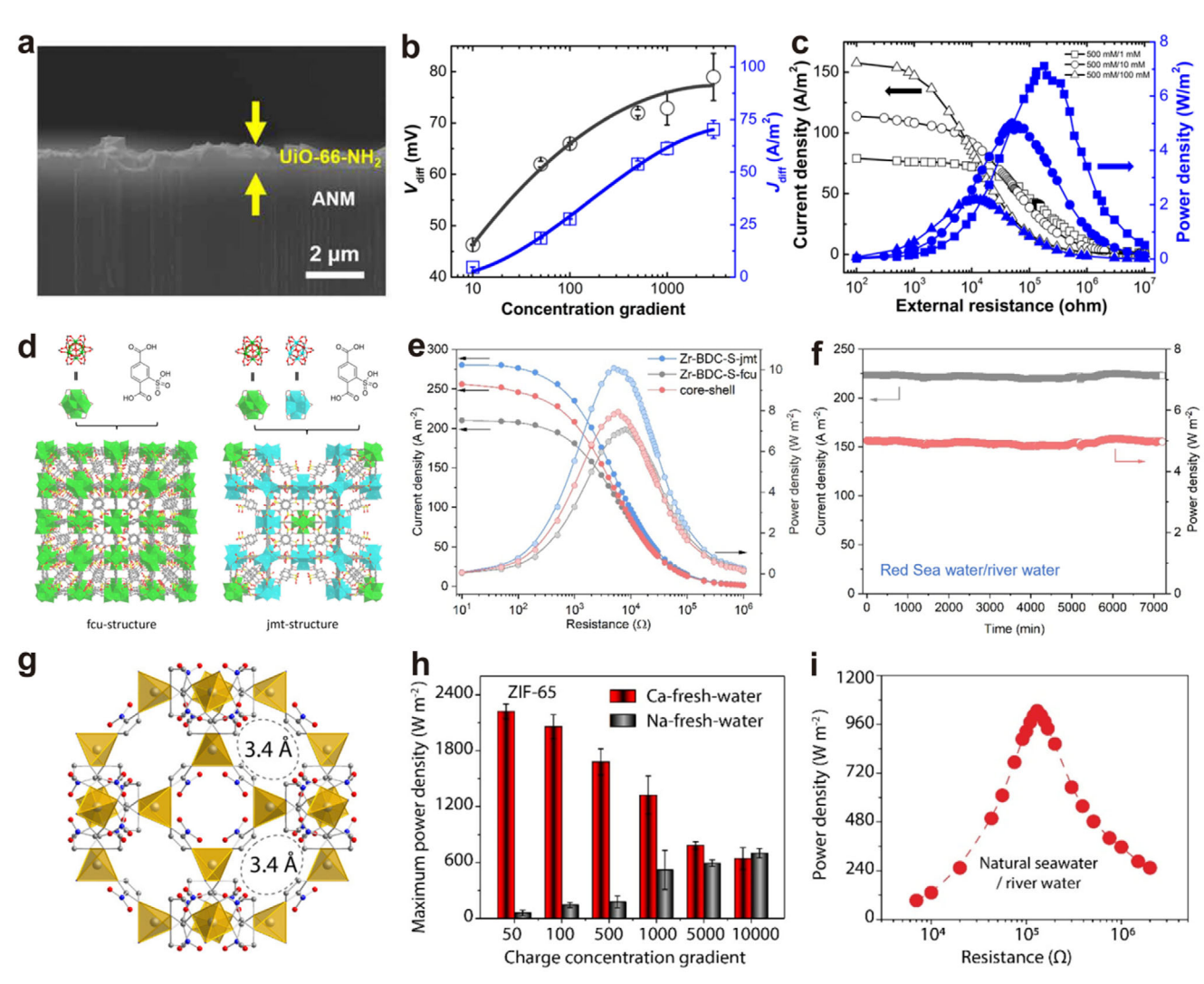


Figure 5. MOFs for osmotic energy harvesting. a) Scanning electron microscope of UiO-66—NH $_2$  layer supported by porous alumina. b) Relationship between diffusion potential ( $V_{diff}$ ), diffusion current ( $I_{diff}$ ), and concentration gradient. c) Relationship between power density, current density, and resistance for UiO-66—NH $_2$  membrane at different KCl concentration gradients. a–c) Reproduced with permission. Copyright 2021, American Association for the Advancement of Science. d) Zr-BDC MOF with different structures, fcu, and jmt. e) Relationship between power density, current density, and resistance for Zr-BDC-S-fcu, Zr-BDC-S-jmt, and their hybrid MOF membrane under a 50-fold NaCl gradient. f) Current density and power density of the Zr-BDC-S-jmt membrane under Red Sea water/0.01 M NaCl solution with 1 kΩ resistance. d–f) Reproduced with permission. Copyright 2024, American Chemical Society. g) Crystal structure of ZIF-65. h) Relationship between maximum power density for ZIF-65 membrane and different concentration gradient. i) Relationship between the power density of ZIF-65 membrane and load resistance under natural seawater and river water. g–i) Reproduced with permission. Copyright 2023, American Chemical Society.

ticles to form a film on anodic aluminum oxide. With an effective testing area of 0.004 mm², such UiO-66—NH $_2$  shows a high Cl $^-$ /SO $_4$  $^2$  $^-$  selectivity of 42.2 and optimal osmotic power of 6.76 W m $^{-2}$  under a 100-fold NaCl gradient (1 M/0.01 M). And methylating imidazole moieties on the UiO-66—NH $_2$  surface can further increase the output power to 10.5 W m $^{-2}$ . Also, the output power density of such UiO-66—NH $_2$  can reach 2.99 W m $^{-2}$  under a 50-fold NaCl gradient, which is comparable to performances of pure UiO-66—NH $_2$  film under the same conditions. In addition, when using UiO-66—NH $_2$  membrane intercalated with poly(sodium-4-styrenesulfonate) (PSS) to support ZIF-8, the heterogeneous MOF membrane could generate a power density of 9.20 W m $^{-2}$  under a 50-fold NaCl gradient. [107] This perfor-

mance enhancement can stem from ion selectivity promotion by ZIF-8 and cation permeability of PSS modified UiO-66—NH $_2$ . Similar polymers-modification strategy was also adopted for HKUST-1. $^{[108]}$ 

An interesting result is that the same MOFs may also demonstrate different osmotic energy conversion efficiency even at the same conditions. For example, a recent study has shown that UiO-66—NH $_2$  layer on porous alumina demonstrates a higher power density of 17.2 W m $^{-2}$  with an effective testing area of 0.03 mm $^2$  under a 50-fold KCl gradient (0.5 M/0.01 M). $^{[109]}$  This result fully hints that the osmotic energy conversion performance of UiO-66—NH $_2$  may be highly correlated with the layer thickness and film orientation. Except for morphology, crystal structures of





www.advmat.de

MOFs would also have a potential influence on the performance. Under some synthetic conditions, some linkers or clusters may miss in UiO-66, even resulting in the formation of some ordered domains across over tens of square nanometers.[110] Based on this fact, influence of other groups, phase and defects of UiO-66 has been studied, which is essential to elucidate their crucial role in improving the efficiency of osmotic energy conversion. In 2024, Chen et al. synthesized Zr-MOFs by using 2sulfonylterephthalic acid (BDC-S) to allow for transformation between the fcu and jmt (Figure 5d).[111] The unit cell length of Zr-BDC-S-fcu is approximately half of that of Zr-BDC-S-jmt and these two sulfonated MOFs both can make cations selective transport. The results show that Zr-BDC-S-jmt membrane with more structure defects has a higher maximum power density (10.08 W m<sup>-2</sup>) than that of Zr-BDC-S-fcu membrane (7.07 W m<sup>-2</sup>) under a 50-fold NaCl gradient (0.5 M/0.01 M) with an effective area of 0.03 mm<sup>2</sup> (Figure 5e). More importantly, the authors used the real seawater from red sea and 0.01 M NaCl to evaluate the current density and output power density. The current density and output power density of Zr-BDC-S-jmt membrane in such media could sustain 225 A m<sup>-2</sup> and 5 W m<sup>-2</sup> in 5 days, respectively (Figure 5f).

In consideration of complex ionic composition of natural water, using 0.5 M and 0.01 M NaCl solution to respectively simulate the real seawater and river water seems to be not rigorous enough because some studies have pointed out that Ca2+ ion is the main ion in the global river, rather than Na<sup>+</sup> ion.<sup>[112]</sup> This also means the actual Na+ concentration gradient between seawater and river water may be higher than 50. Regarding this issue, Li et al. attempted to develop MOFs with high Na<sup>+</sup>/Ca<sup>2+</sup> selectivity for osmotic energy harvesting.<sup>[113]</sup> They selected ZIF-65 crystals to construct Na<sup>+</sup> channels by filling ZIF-65 crystals in a glass micropipet to perform diffusion-drift experiment (Figure 5g). It has been discovered that ZIF-65 crystals enable Na+ transport but reject Ca<sup>2+</sup> ions. By using molecular dynamics (MD) calculation, the -NO<sub>2</sub> groups in ZIF-65 can lower the Na<sup>+</sup> dehydration barrier by providing coordination, thereby facilitating Na<sup>+</sup> transport. But due to the larger hydration shell for Ca<sup>2+</sup>, such effects for dehydration is far insufficient to make Ca<sup>2+</sup> dehydrate, and thus Ca<sup>2+</sup> transport in ZIF-65 is hindered. Furthermore, ZIF-65 membrane (7 mm<sup>2</sup>) supported by aluminum oxide demonstrates maximum output power densities of 2221 and 1858 W m<sup>-2</sup> at the 50-fold concentration gradient (0.5 M/0.01 M) for NaCl/Ca(HCO<sub>3</sub>)<sub>2</sub> and NaCl/CaCl<sub>2</sub> solution, respectively (Figure 5h). In natural river water and seawater, the maximum output power densities can reach 1027 W m<sup>-2</sup>, as displayed in Figure 5i. This is the best performance of MOF under current real water conditions. The reason why there is an order of magnitude improvement in power density is that the concentration gradient for Na<sup>+</sup> ions is much higher than 50 and the ZIF-65 can transport Na+ ions but almost completely reject Ca<sup>2+</sup> ions due to Ångström-scale pore size and neutral ligands. Apart from natural salinity gradient, it is also desirable to explore other influencing environment factors. For instance, Xia's group proposed a strategy that utilizes light energy to enhance energy conversion performance of the MOF membrane.[114] In order to make full use of natural light, they selected 5,10,15,20-tetra(4-carboxyphenyl)porphyrin (TCPP) ligand to fabricate ZnTCPP MOF on porous aluminum oxide owing to the high photoactivity of TCPP ligand. The authors observe that the ZnTCPP MOF possesses cation selectivity and the open circuit voltage remains the same while the short circuit density increases as the light power density increases. Moreover, at a 3000 fold KCl salinity gradient (3 M/1 mM) and an effective area of 0.1256 mm², the light irradiation could elevate the power density to 7.74 W m $^{-2}$ , a significant increase from 6.26 W m $^{-2}$  observed under dark condition. Similar research has also been reported on CuTCPP MOF.  $^{[115]}$ 

Apparently, ion-selective transport is the determining characteristic for framework materials' ability to perform performance in osmotic energy conversion. In principle, MOFs with anionic or cationic selectivity always exhibit certain osmotic energy conversion performances when using the MOF membrane to separate the prepared salt solution with gradients. Similar to the study on ion selectivity in nanochannels, researches on MOFs-based osmotic energy harvesting also mainly focus on UiO-66 and its derivatives while insufficient attention has been paid to other MOFs. The above research results reflect an important point that the film orientation and thickness, crystal structures, defects and chemical groups of MOFs have obvious effects on the osmotic energy harvesting performances, but the dominant structure factor and influence trend is still not clear. Especially for MOFs film orientation on porous substrate, it may form by the accumulation of completely disordered polycrystals. And the film is hard to control and would exhibit completely different orientation under different solvent thermal conditions. These factors also result in only a small portion of MOF materials exhibiting extremely high performance. Another issue that needs more attention is the actual salinity between river water and seawater. This specific value may significantly vary in different geographical environment, and thus the cations and anions concentrations in real river water and seawater should be measured with some accurate analytical method, such as ion chromatography. The osmotic energy conversion performance of MOFs evaluated at actual gradient is more meaningful in a real-water context.

#### 3.2. COFs for Osmotic Energy Harvesting

The preparation strategy of COF membrane on porous substrate and the evaluation method for their osmotic energy harvesting performances is basically the same as those of MOF materials. Many COFs perform on par with that of MOFs in osmotic energy harvesting. Some COF membranes can also yield an output power density higher than 5 W m<sup>-2</sup> under a 50-fold NaCl or KCl salinity gradient.[116,117] It is noteworthy that, in 2022, Lai's group first realized high osmotic energy conversion performances by using a couple ion-permselective oriented COF membranes. [118] In their research work, sulfonate groups (SO<sub>3</sub>H) and quaternary ammonium (QA) groups were introduced to synthesize two types of COF membranes (COF-SO<sub>3</sub>H and COF-OA) for K<sup>+</sup> and Cl<sup>-</sup> transport, respectively (**Figure 6a**). Taking porous SiN<sub>x</sub> as the support, the COF-SO<sub>3</sub>H and COF-QA membranes were assembled into a pair and tested with a dynamic flow cell (Figure 6b). Under a 50-fold NaCl gradient (0.5 M/0.01 M), the maximum power density could reach 43.2 W  $m^{-2}$  when the COF membrane is 0.1 µm thick with an effective area of 0.03 mm<sup>2</sup>. More importantly, the orientation of COF nanochannels has been proven to have a significant impact on power density.

15214095, 0, Downloaded from https://advanced.onlinelibrary.wiley.com/doi/10.1002/adma.202501881 by HONG KONG POL YTECHNIC UNIVERSITY HU NG HOM, Wiley Online Library on [26.09/2025]. See the Terms

and-conditions) on Wiley Online Library for rules of use; OA articles are governed by the applicable Creative Commons

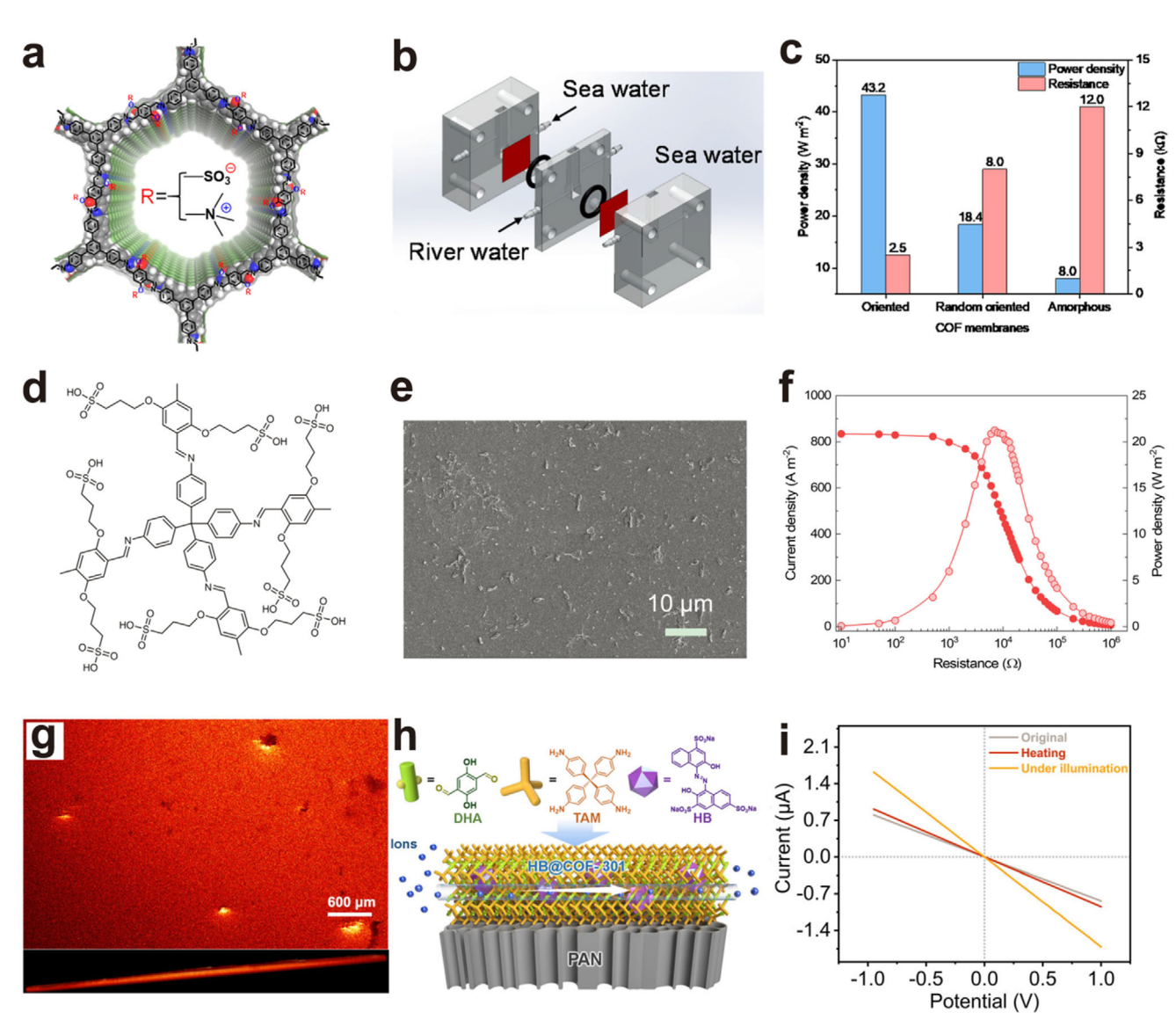


Figure 6. COFs for osmotic energy harvesting. a) Structure of COF-SO<sub>3</sub>H and COF-QA. b) Schematic diagram of flow cell for the measurement of osmotic energy conversion by using COF membranes. c) Relationship between power density, resistance, and oriented degree of COF-SO<sub>3</sub>H/COF-QA membranes. a–c) Reproduced with permission.<sup>[118]</sup> Copyright 2022, American Chemical Society. d) 3D COF structure. e) Scanning electron microscope image of dense 3D COF membrane. f) Current density and power density of 3D COF membrane influenced by external resistances at a 50-fold concentration gradient. d–f) Reproduced under the terms of the CC-BY Creative Commons Attribution 4.0 International license.<sup>[122]</sup> Copyright 2023, T. Zhu et al., published by Springer Nature. g) Confocal microscopy image of the COF-301 membrane with HB. h) Hybrid structure of COF-301 membrane. i) Current-voltage measurement in 1 M KCl under heating and illumination. g–i) Reproduced under the terms of the CC-BY Creative Commons Attribution 4.0 International license.<sup>[123]</sup> Copyright 2023, Q. Guo et al., published by Springer Nature.

With the increasing nanochannel orientation, the power density drastically increases and resistance greatly decreases, as shown in Figure 6c. Also, the membrane thickness has been found to influence the power density. When the thickness increases to 1  $\mu m$ , the power density decreases to 12.5 W m $^{-2}$ . In addition, in Red Sea/river water and Dead sea/river water, the maximum power density could be up to 28.9 and 228.9 W m $^{-2}$ , respectively. And eleven COF membrane units in series connection can offer a 1.6 V voltage output. Such performances in series connection are the highest osmotic energy conversion in COF-based materials. Given the influence of COF membrane

thickness, a monolayer COF membrane is expected to show a lower membrane resistance and higher osmotic energy conversion performances. In order to study this, in Yang's work, a monolayer COF (1.1 nm) composed of zinc tetraphenylporphyrin (ZnTPP) and 2,5-dihydroxyterephthalaldehyde (DHTA) was successfully constructed on the silicon nitride with a single 2- $\mu$ m-wide aperture. The results show that this ultrathin membrane (3.14  $\mu$ m2) can produce output power density of 294.3 W m $^{-2}$  in a China's Yellow Sea/Yangtze River water gradient. This work fully reveals the structure advantage of COF monolayer.



ADVANCED MATERIALS

www.advmat.de

High osmotic energy harvesting performances of 2D COF membranes have further stimulated researcher's interest in the exploitation of 3D COFs because narrower pore sizes and more interconnected channels in 3D networks may enhance selective ion transport efficiency. However, only a few 3D COF membranes have been reported so far.[120,121] The difficulties in synthesis of 3D COFs mainly stem from larger steric hindrance for assembly of tetrahedral building blocks. Notably, in 2023, Jiang's group first studied the selective ions transport behavior and osmotic energy conversion performance of 3D COFs.[122] They used tetra-(4-anilyl) methane and sulfonic acid-functionalized aldehyde as monomers to successfully prepare dense membrane based on side-chain sulfonic acid-functionalized 3D COFs by using dual acid-mediated interfacial polymerization approach, as exhibited in Figure 6d,e. The pore size of this 3D COF is  $\approx$ 0.98 nm, which is smaller than that of normal 2D COF. Surprisingly, this 3D COF membrane supported by a polyacrylonitrile substrate shows cation selectivity, as revealed by current-voltage measurements. And the maximum power density for this 3D COF membrane with an effective area of 0.03 mm<sup>2</sup> could reach 21.2 W m<sup>-2</sup> under 50-fold NaCl concentration gradient (0.5 M /0.01 M) when the load resistance is 7 k $\Omega$  (Figure 6f). Although the maximum power density is not at a high level but the energy conversion efficiency of 3D COF membrane is up to 45.3%, which is also the highest level among the COFs.

Apart from dimensionality of COFs, how to introduce solar energy to improve the performances of COFs is also an intriguing topic in osmotic energy harvesting. A highly attractive strategy is to construct ionic COF membranes with photoelectric responsiveness to generate photo-induced ion movement, which facilitates amplifying the osmotic energy harvesting performances. In 2023, Guo et al. employed dyes to introduce into COF membrane as guest molecules for generating photoelectric responses because dyes have excellent photoresponsive properties.[123] The specific method is to use 2,5-dihydroxyterephthaldehyde (DHA) and tetrakis(4-aminophenyl)methane (TAM) to synthesize 3D COF-301 for encapsulating hydroxynaphthol blue (HB) molecules (Figure 6g,h). By adjusting the HB concentration in the initial reaction, the HB loading in COF-301 can be wellcontrolled and such HB incorporated COF-301 membrane is cation selective. Interestingly, the ion screening capabilities of COF-301 membrane could be greatly influenced by the HB contents, as revealed by the cation transfer number calculation. Ion permselectivity would increase when the HB content in COF-301 increases to 0.324 mmol g<sup>-1</sup>. Upon light exposure, the whole membrane conductance has been observed to increase, which is a result of proton-coupled electron transfer for HB molecules. This phenomenon indicates that the surface charge density of the COF-301 pore channel can be regulated by light exposure, further influencing the ion selectivity. As for the performances, the open circuit potential of COF-301 membrane (4 mm×1.5 mm) could increase to 150 mV from 147 mV and the short circuit current could increase to 0.34 µA from 0.20 µA under light exposure. The maximum output power density could reach 129 W m<sup>-2</sup> under 50-fold NaCl concentration gradient (0.5 M/0.01 M). This work provides valuable reference for light-assisted osmotic energy harvesting.

So far, the COF material with the optimal performances in osmotic energy harvesting is the Ca-COF membrane.[124]

In this work, an axial orientation strategy has been proposed for constructing metal-COF membranes with precisely organized nanochannels. The authors selected 2.4.6triformylphloroglucinol (TP) and triaminoguanidinium chloride (TG) as monomers to synthesize COF membrane by interfacial polymerization, followed by the coordination of a series of metal ions including Ca<sup>2+</sup>, Mg<sup>2+</sup>, Co<sup>2+</sup>, Cu<sup>2+</sup>, Zn<sup>2+</sup>, Al<sup>3+</sup> and Fe<sup>3+</sup>. In these COFs, these coordinated metal ions act as molecular bridges and could connect COF framework layers through O and N atoms, which induces parallel arrangement for COF layers. Thus these COFs have axial alignment and the channels are highly oriented. Among all these metal-COFs, the Ca-COF membrane (effective area 10<sup>-4</sup> mm<sup>2</sup>) delivers an impressive output power density of 180.5 W m<sup>-2</sup> under a 50-fold NaCl gradient (0.5 M/0.01 M), which is  $\approx$ 190% higher than that of the COF membrane without the Ca metal. The Ca-COF membrane could exhibit a maximum output power density of 320.8 W m<sup>-2</sup> using seawater (Yellow Sea in China) and river water (Beihang University's inlands water). For other metal ions coordinated COFs, the output power densities are also twice as high as those COF membranes without metal ions. This work highlights the importance of nanochannel orientation in COF membranes for boosting osmotic energy.

Regarding chemical groups, structural dimensionality, guest molecules and film thickness and orientation, in contrast, current research on COF membranes-based osmotic energy harvesting is more detailed than that of MOFs. It can be expected through optimizations of these influencing factors, the performances for osmotic energy harvesting of COF membranes could reach a higher level. Indeed, it is a challenging task because balancing dimensionality and nanochannel orientation during COFs synthesis is not easy. For the current leading COF material (Ca-COF) in osmotic energy harvesting, the reason why calcium, instead of other metal ions, yields optimal performance remains elusive. Essentially, the axial orientation of the nanochannels in COF is fairly consistent after introduction of different metal ions. The structure-performance relationship in this case is not fully understood and may be related to the coordination number and structure. On the other hand, introducing some guest molecules into COF membranes for using light to enhance performances also bring much uncertainty in distribution, conformation and contents. Meanwhile, some factors also seem to constrain each other. For example, an increase in the complexity of the COF structure will lead to an increase in the tortuosity of the channels, which is favorable for enhancing ion transport selectivity. But this also may increase the transport resistance of targeted ions, resulting in a decrease in energy conversion efficiency. Therefore, finding a balance among these performanceinfluencing factors is very important to realize the high efficiency of COFs in osmotic energy conversion. So far we are not yet able to predict the performance upper limits of COFs in osmotic energy harvesting according to existing experimental conditions. Using industrial standard as a benchmark, a specific power density of 5 W m<sup>-2</sup> has been proposed by considering the membrane lifespan, actual operating conditions, and economic feasibility.[125] Although the maximum output power of most MOFs and COFs has already exceeded this value, the cost and lifespan of the membranes remain as the limitations in industrialization. As for introducing other energy source such

15214095, 0, Downloaded from https://advanced.onlinelibrary.wiley.com/doi/10.1002/adma.202501881 by HONG KONG POLYTECHNIC UNIVERSITY HU NG HOM, Wiley Online Library on [2609/2025]. See the Terms and Conditions (https://onlinelibrary.wiley.

com/terms-and-conditions) on Wiley Online Library for rules of use; OA articles are governed by the applicable Creative Commons I

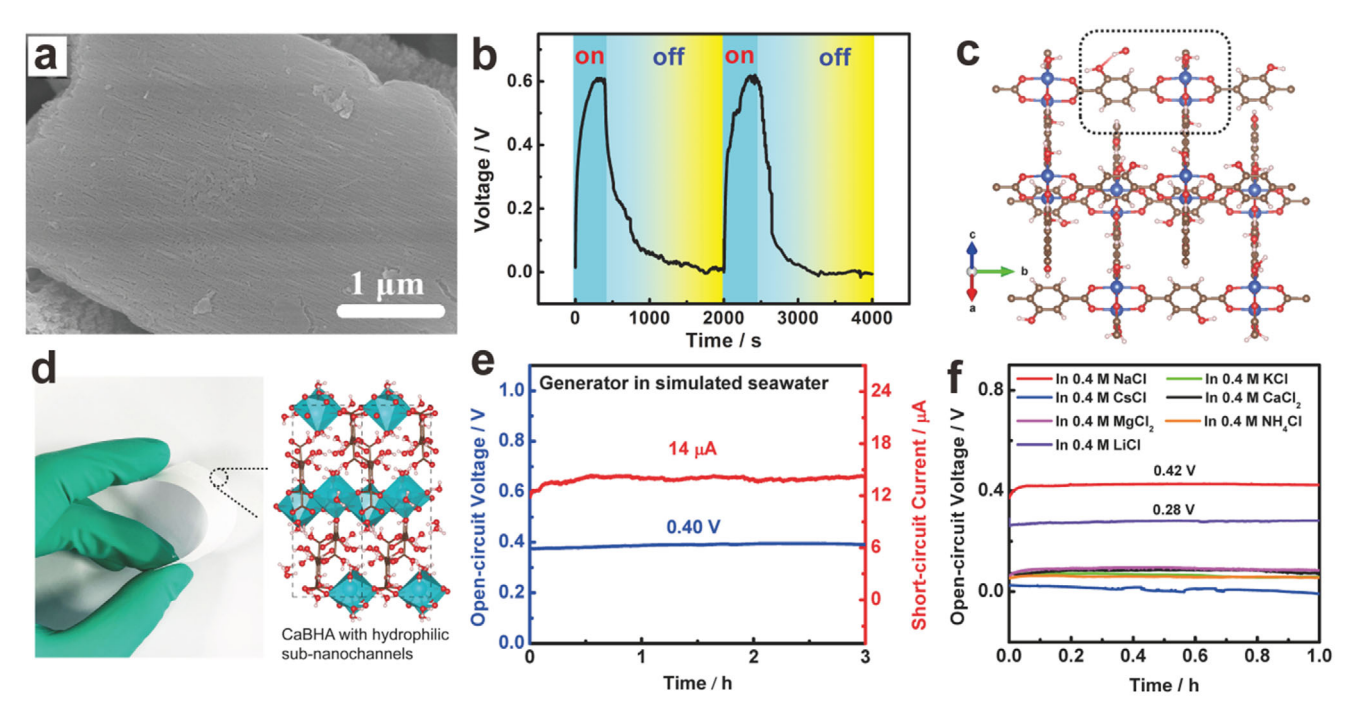


Figure 7. Water and seawater evaporation induced electricity generation with MOFs. a) Scanning electron microscope image of hierarchical oriented Cu(BDC—OH) assemblies. b) Open circuit voltage on and off for Cu(BDC—OH) based generator with opening and closing test container. c) OH<sup>-</sup> adsorption by —OH group in Cu(BDC—OH) after geometry optimization with DFT calculation. a–c) Reproduced with permission.<sup>[128]</sup> Copyright 2021, Wiley. d) Hydrophilic CaBHA single crystals supported by CaCO<sub>3</sub> paper. e) Open circuit voltage and short circuit current of CaBHA generator under simulated seawater evaporation at steady state. f) Open circuit voltage and short circuit current of CaBHA generator in different salt solutions at steady state. d–f) Reproduced with permission.<sup>[130]</sup> Copyright 2024, American Chemical Society.

as light, the current efficiency has still not improved in the order-of-magnitude, warranting a need for future research in this direction.

### 4. Evaporative Energy Harvesting

Research on water evaporation induced electricity generation was first reported in the year of 2017. The carbon black with abundant oxygen groups was found to be capable of generating an open circuit voltage of 1 V under continuous natural water evaporation.[20] In 2020, some MOF-related works on harvesting electricity induced by water evaporation started to emerge. These studies focus on fabricating the MOF hybrids such as UIO-66/AlOOH, Cu-CAT/gelatin and polyaniline-coated MOFs for exploration of performances in electricity generation, [23,126,127] rather than pure MOFs. These MOF hybrids also show high voltage induced by water evaporation. In 2021, Wang et al. first realized water evaporation induced electricity harvesting by using pure MOFs and explored the influencing factors including wind speed and humidity.[128] In this work, 2-hydroxybenzene-1,4-dicarboxylic (H<sub>2</sub>BDC-OH) and Cu(OH)<sub>2</sub> as the ligand and Cu sources were adopted to grow Cu(BDC-OH) MOF on the robust CaCO3 paper. A hierarchical oriented assembly strategy was used to make 1D channels of Cu(BDC-OH) to arrange into ordered and long-range pattern (Figure 7a), for generating a stronger electrokinetic effect, namely, hydrated proton flow. It is interesting that such Cu(BDC-OH) MOF-based generator (12 cm<sup>2</sup>) can generate a voltage of 0.6 V and 0.12 μA in the pure water under natural evaporation. And the open circuit voltage can be controlled by periodically sealing and unsealing the system for inhibiting the water evaporation (Figure 7b). Finite elements simulation results confirm that the surface charge density is an important physical factor of the materials determining the electricity generation. Further study results show that Cu(BDC) without —OH groups exhibits a voltage of 0.3 V, fully manifesting that —OH groups in Cu(BDC—OH) MOF play a dominant role in increasing the surface charge density. Density function calculation results of OH $^-$  adsorption on —OH groups (–0.61 eV) in Cu(BDC—OH) show a more negative energy difference than  $\rm H_2O$  adsorption (–0.23 eV) (Figure 7c), manifesting a tendency to adsorb OH $^-$ , instead of  $\rm H_2O$ . This is essential to improve the average surface charge density, further enhancing the voltage.

Currently, the optimal evaporation induced electricity generation performance of pure MOFs in pure water is held by MOF-801. The open circuit voltage and short circuit current can be up to  $\approx\!0.7$  V and 0.7  $\mu A$  at room temperature with a relative humidity of 44%. And the generator voltage based on MOF-801 small nanocrystals can reach 2 V at 32 °C with a low relative humidity of 28%. Since vapor pressure is the driving force, all factors affecting evaporation such as wind, humidity and temperature will influence the electricity generation performance. But limited by the finite fresh water resources, harvesting electricity by using seawater evaporation demonstrates much more practical significance due to immense reserves of seawater. However, seawater contains elevated concentration of ions, which would significantly weaken the electrokinetic effect and thus cannot





www.advmat.de

generate electricity in general cases. To tackle this formidable challenge, in 2024, Wang et al. further proposed a concept of unipolar solution flow and designed a new Ca based MOF to achieve high performances in seawater evaporation induced electricity generation.<sup>[130]</sup> The new CaBHA MOF composed of Ca ions and benzenehexacarboxylic acid (BHA) supported by CaCO<sub>3</sub> paper is superhydrophilic (Figure 7d), which is determined by abundant -COOH groups. It is gratifying that CaBHA based generator (12 cm<sup>2</sup>) could yield a voltage of 0.4 V and a current of 14 µA under natural evaporation of simulated seawater (Figure 7e), which is at the best performance level in the salt solution induced electricity generation. And the current of parallel connection of 72 CaBHA based generators can reach 1 mA. Such outstanding performances originate from selective transport of Na<sup>+</sup> in the subnanochannels (Figure 7f) to generate a streaming potential, which is related to hydrogen bond network structure in CaBHA. And other cations flow in the CaBHA nanochannels only generates a lower potential than Na+, indicating that CaBHA nanochannels possess cations selective properties. This research work fully demonstrates the superiority of the Ca-MOF in the high performances of seawater evaporation induced electricity generation.

Unfortunately, COF materials are still unexplored in this field. As of now, no study on pure water or seawater induced water evaporation energy generation by using COF has been reported. On the other hand, there is also not much research on using MOFs to harvest evaporative energy from water. It is also imperative to be acknowledged that the research on MOFs-based water evaporation induced electricity generation is still in its early stages although some important breakthroughs have been made. On the basis of the current state of research, we can make a conclusion from the finite element simulation results that the streaming potential increases with surface charge density in an ideal state. But it is still unknown which level the maximum surface charge density of MOFs in water can reach in a practical situation. Therefore, setting aside environmental factors such as water quality and evaporation conditions, we are still unable to predict the maximum electrical energy generated by water evaporation based solely on the surface charge density of the MOFs. The root cause lies in our relatively shallow understanding of the formed electric double layer in framework materials in water. In the context of regulating the overall structure of electrical double layer for MOFs in pure water, developing and controlling mesoporous structures within MOF crystals presents a highly promising approach. In recent years, various mesoporous MOFs have been successively reported, garnering extensive attention due to the tunable pore structure and high surface area.[131-134] These mesoporous MOFs exhibit considerable diversity and adaptability in their mesostructures, offering many possibilities in enhancing surface charge density in pure water. It is conceivable that more oxygen-containing groups or units may be exposed within the constructed mesoporous structure channels, facilitating the formation of a negatively charged compact layer. On the other hand, the mesopores in MOFs, acting as capillary channels, are more favorable for water transport due to their lower flow resistance compared to intrinsic micropores. Additionally, the electrical double layer configuration has been found to be affected by convection, as reflected by surface conductivity.[135] This also manifests the electric double layer structure of framework materials may be completely different when the water is in a static state compared to when it is in a dynamic flow state. Overall, it is necessary to clearly analyze the specific structure of the compact layer of framework materials in water and complex saline water under flow conditions. This will aid in the exploration of maximizing the electricity generation performance of MOFs, as well as COFs. Certainly, as this field is still in its early stages, there are no widely recognized performance benchmarks yet, which are expected to be established in the future.

## 5. Perspectives

#### 5.1. Deep Study on Framework Materials-Based Nanofluidics

Ion-selective transport behavior in nanochannels dominates the performances of framework materials in targeted ion extraction, osmotic and evaporative energy harvesting. The corresponding relationships, properties, and performances of MOFs and COFs have been summarized in Table 1. Current research indicates that MOFs exhibit higher selectivity in F<sup>-</sup> and Na<sup>+</sup> ion extraction whereas COFs show superior selectivity in Li<sup>+</sup> ion extraction. In terms of osmotic energy harvesting, MOFs exhibit higher output power density but COFs demonstrate higher performance durability. As for evaporative energy harvesting, MOFs are in a leading position, while there is a research gap in COF materials. Overall, MOFs and COFs also exhibit similar advantages and limitations. Concerning the advantages, the framework materials not only have high ion-selectivity and tunable subnanopore and nanostructure, but also have the capability to be assemblable and integrable. However, their limitations include the lack of universal methods for large-scale and precise production, moderate mechanical strength and relatively poor longevity compared to the commercial membranes. The analysis reveals that both the merits and constraints of the framework materials are fundamentally rooted in their selectivity and structural stability. To fully leverage the advantages and overcome the limitations, the primary focus should be on a deep study on framework materials-based nanofluidics.

On the realization and regulation of ion selective transport, the general strategy is selecting a target MOF or COF as the study subjects and introducing some acid (-SO<sub>3</sub>, -PO<sub>3</sub>, -COO) or base (-NH<sub>2</sub>) groups, or small molecules and metal ions into the ligand, to greatly influence the selective ions movement under external fields. This ion selectivity essentially relies more on steric hindrance and Coulomb blockade in narrow channels caused by these groups and molecules. Actually, as displayed in Figure 8a, the cations have highly close hydrated diameter (D<sub>H</sub>),[136] and the cation selectivity of most framework materials has yet to reach the level of natural protein ion channels. It is noteworthy that extremely precise ion separation of natural Na<sup>+</sup> and K<sup>+</sup> ion channels is achieved by minute differences in ions solvation behavior,[137] which is completely determined by ultra-fine protein structure. In these structures, the spacing and arrangement of oxygen groups have a significant impact on achieving subtle solvation effects. In comparison, the channel structures of framework materials appear overly simplistic, even some molecules or groups are incorporated into the pores. This also results in the generally poor selectivity between monovalent ions for framework materials. Therefore, it is a necessity to

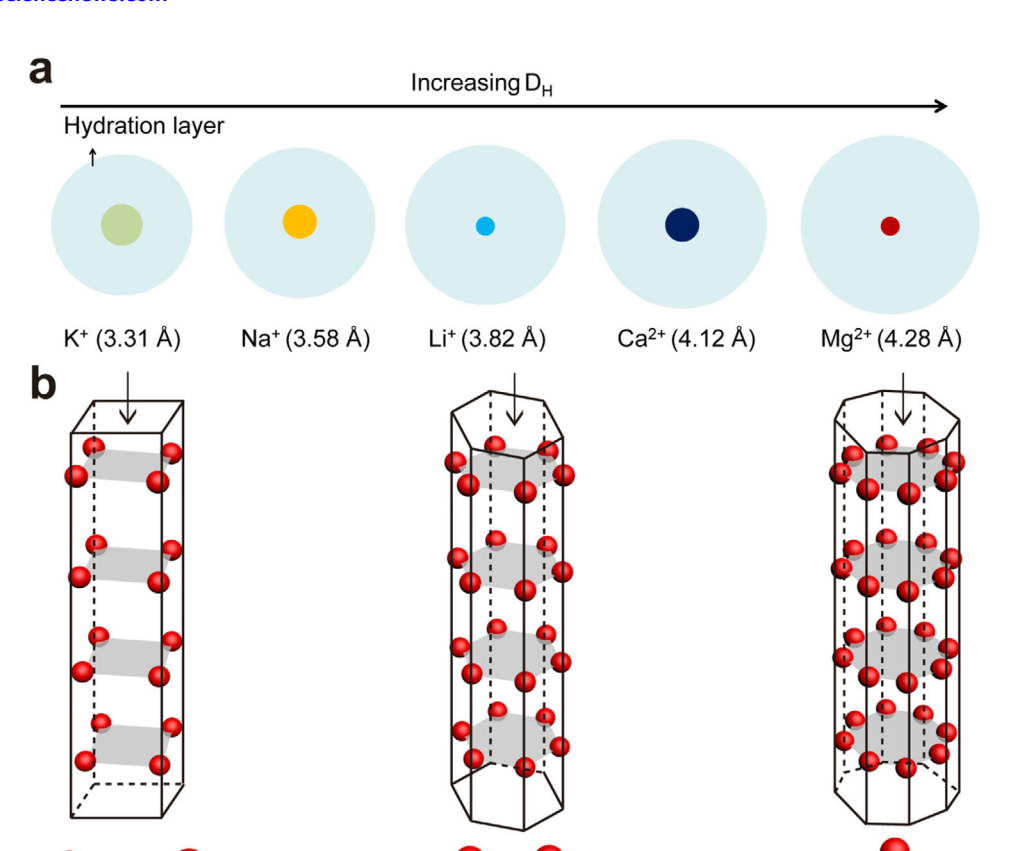


Table 1. Relationship among ion extraction, osmotic energy harvest, and evaporative energy harvest and corresponding features of MOFs and COFs.

MOFs	Ion extraction	Osmotic energy harvest	Evaporative energy harvest
Driving force	Primarily electric field	Osmotic pressure	Capillary force and vapor pressure
Channel size	Ångström scale	Sub-nano or nanoscale	Nanoscale or microscale
Ions selectivity	Predominantly cationic (Li $^+$ , Na $^+$ and K $^+$ ), seldom anionic (F $^-$ )	Predominantly cationic (Na <sup>+</sup> and K <sup>+</sup> )	Proton-transport in pure water, seldom cationic in saltwater
Current optimal performances	and Na <sup>+</sup> /Li <sup>+</sup> = 1770.0 (15C5-UiO-66-(COOH) <sub>2</sub> ),	ximum output power density: 2221 W m <sup>-2</sup> for NaCl/Ca(HCO <sub>3</sub> ) <sub>2</sub> at 50-fold concentration radient, 71.6 and 1027 W m <sup>-2</sup> for 50-fold NaCl concentration gradient and seawater/river water, respectively (ZIF-65)	Open circuit voltage and short circuit current: 0.7 V and 0.7 $\mu$ A in pure water (MOF-801), 0.4 V and 14 $\mu$ A in simulated seawater (CaBHA)
Performance duration	Up to 30 days	Over 5 days	Over 5 days
Advantages	High ion selectivity, tunable subnanopore and nanostructures, assemblable and integrable		
Limitations	Lack of universal methods for large-scale and precise production, moderate mechanical strength, relatively poor longevity		
COFs	lon extraction	Osmotic energy harvest	Evaporative energy harvest
	lon extraction Electric field or pressure	Osmotic energy harvest Osmotic pressure	Evaporative energy harvest  Capillary force and vapor pressure
Driving force			Capillary force and vapor
COFs Driving force Channel size Ions selectivity	Electric field or pressure	Osmotic pressure	Capillary force and vapor pressure
Driving force Channel size Ions selectivity	Electric field or pressure  Sub-nano or nanoscale	Osmotic pressure  Sub-nano or nanoscale  Predominantly cationic (Na <sup>+</sup> and K <sup>+</sup> ), seld  anionic (Cl <sup>-</sup> )	Capillary force and vapor pressure  - lom -  m <sup>-2</sup> -  nt,
Driving force  Channel size  Ions selectivity  Current optimal  performance	Electric field or pressure $Sub\text{-nano or nanoscale}$ $Predominantly \ cationic\ (Li^+,\ Na^+\ and\ K^+)$ $Ion\ selectivity\ at\ molar\ ratio\ of\ 1:\ K^+/Na^+=1.7\ and\ Na^+,$	Osmotic pressure  Sub-nano or nanoscale  Predominantly cationic (Na <sup>+</sup> and K <sup>+</sup> ), seld anionic (Cl <sup>-</sup> )  (K <sup>+</sup> Maximum output power density: 180.5 W r for 50-fold NaCl concentration gradien 320.8 W m <sup>-2</sup> for seawater/river water	Capillary force and vapor pressure  - lom -  m <sup>-2</sup> -  nt,
Driving force Channel size Ions selectivity Current optimal	Electric field or pressure $Sub-nano\ or\ nanoscale$ $Predominantly\ cationic\ (Li^+,\ Na^+\ and\ K^+)$ $Ion\ selectivity\ at\ molar\ ratio\ of\ 1:\ K^+/Na^+=1.7\ and\ Na^+,$ $=2.7\ (COF-Cys),\ Li^+/Mg^{2+}=321\ (COF-300-CH_{0.6})$ $-$	Osmotic pressure  Sub-nano or nanoscale  Predominantly cationic (Na+ and K+), seld anionic (Cl-)  (K+ Maximum output power density: 180.5 W r for 50-fold NaCl concentration gradien 320.8 W m-2 for seawater/river water (Ca-COF)	Capillary force and vapor pressure  - lom -  -  n <sup>-2</sup> -  pt,

optimize existing structures of framework materials or creating new ones with a structure closer to natural ion channels, in order to exploit minute differences in solvation and achieve higher ion selectivity. The arrangement and positions of oxygen atoms in nanochannels of framework materials are crucial because they will lead to minute differences in coordination interaction for solvated cations. The most important yet challenging task in the future is the design of framework materials with Li<sup>+</sup> ion channels. This is due to the strategic importance of Li in battery industry and absence of natural Li+ ion channels for us to take as reference. Further simulations for Li<sup>+</sup> ion channels still have to rely on Na<sup>+</sup> ion or K<sup>+</sup> ion channels as reference. Additionally, the hydrolytic stability of the framework material must be taken into account and strong field ligands may be required to resist dissociation in water, because of potential channel collapse triggered by capillary force. [138] From these perspectives, it can be envisioned that an ideal framework material for ion extraction and osmotic harvesting should have stable and continuous or subnano-sized channels, which is constructed by oxygen atoms with different geometric configuration (Figure 8b). These channels have precise oxygen distance to allow minute differences in cation solvation and demonstrate high ions transport selectivity under pressure or electric field. For evaporative energy harvesting, the size of oxygen-rich channels can be expanded from sub-nanometer to nanometer scale for further enhancing the flux of water flow. In addition to the crystal structures, some other factors influencing nanofluidics including film orientation, thickness, and area also needs to be systematically studied to give an optimal range.

Another issue is that there are critical knowledge gaps in our understanding of ion solvation, water transport and charged behavior in channels of framework materials. In this regard, characterization techniques and computational modeling are equally important. Although some useful analytical techniques such as in situ small-angle X-ray scattering, [139,140] ambient pressure Xray photoelectron spectroscopy,[141] and Raman spectroscopy,[142] have been used to probe confined interaction on solid-liquid interfaces of carbon materials, research on this aspect of framework materials is still a blank. The interaction between the confined space of the framework material and water, as well as ions, needs to be further studied. In addition, in situ liquid time-of-flight secondary ion mass spectrometry is a powerful tool to investigate ion transport mechanism.[143,144] The quadrupolar solid-state NMR spectroscopy is an effective method for capturing the features of water in subnanochannels.[145] And charge profiling 3D atomic force microscopy would provide significant assistance in quantifying the real-space charge distribution of the material surface with angstrom depth resolution in solution,[146] which is crucial for exploring the interfacial electric double layer of framework materials in different solutions. These physical characterization techniques will help us understand the transport mechanisms of ions and water, for elucidating the differences in ion selectivity in nanochannels of framework materials. Particularly, because



Different subnanochannels constructed by oxygen atoms

cation

Figure 8. Hydrated ion size and the conceptualized oxygen channels for ion-selective transport. a) Different hydrated cations with highly close hydrated diameter (DH). b) Three conceived subnanochannel structures in framework materials constructed by oxygen atoms for selective cation transport. The red balls represent oxygen atoms. In these channels, different number of oxygen atoms in a plane can provide different coordination to cations and result in minute differences in cations solvation, which may be the key to enhance recognition of monovalent ions.

O atom

local dielectric constant would change and may influence the ion solvation and water self-dissociation, [147] understanding the dielectric property of water in confined space of MOFs and COFs is highly necessary. The experimental evidence suggests that dielectric constant of water confined at the hexagonal boron nitride nanochannel would be low down to 2, which is much smaller than that of bulk water (≈80).<sup>[148]</sup> This measurement result also hints that the dielectric property of water would be also strongly suppressed in the nanoconfined space in framework materials. It could be predicted that the dielectric constant of water in framework materials might be also low, and experimental efforts in this area are lacking.

Except for characterization, theoretical calculations focusing on confinement are also important. Molecular dynamic simulation is widely used in water and ion transport at nanoscale, [149,150] which is also helpful to explain and analyze some phenomena in ion selectivity such as adsorption and transport. In this aspect, the selection of the force field should be more cautious, as the movement of ions under pressure-driven and electric field-driven conditions may differ because of different interactions. Specifically, different type of driving force may result in different dehydration and transport-based energy barriers for ions, which means there are differences in ion dehydration, adsorption and selective transport behavior under pressure and electric field. Such differences may be more pronounced, especially for those framework materials with stronger metallic properties because they would be polarized under an electric field to provide a different conformation. Thus, for an electrical field-driven condition, a polarizable force field may be more appropriate than a nonpolarizable one. Of course, both of nonpolarizable and polarizable force field cannot capture all physical effects so some new force fields also need to be reasonably designed and developed. Besides the force field, some well-established atomistic water models such as polarizable water models and rigid nonpolarizable water models may



www.advmat.de

need to be reconsidered to better describe a particular physical property in the case of simulations in framework materials, especially for the dielectric constant. As mentioned above, the dielectric constant of water would be anomalously low in nanoconfined spaces. Further clarification is needed on the impact of electric fields on the behavior of confined water in channels of framework materials, as this could significantly affect the ion selectivity. In the study of nanofluidics in framework materials, some classical physical equations may need to be modified or some classical theories may no longer hold. For example, the breakdown of the Nernst-Einstein relationship has been confirmed in 0.8 nm carbon nanotubes. [151] From a theoretical perspective, this also presents an opportunity to establish new physical laws in nanofluidics.

#### 5.2. Normalization of Test Conditions

To ensure the comparability and reliability of performance results in the future research and development of technologies, it is crucial to employ consistent conditions and methodologies. While certain testing conditions, such as concentration gradients, are widely accepted, there remains a lack of standardization in specific test conditions in targeted ion extraction, osmotic and evaporative energy harvesting. In the context of ion extraction, ion selectivity stands out as a critical performance metric, which is typically assessed using chlorate salts as the feeding solution under electrical field or pressure. The equation of computing selectivity ( $\alpha_{ii}$ ) is as follows:

$$\alpha_{ij} = \frac{J_i/\Delta C_i}{J_i/\Delta C_i} \tag{1}$$

where  $\Delta C_i$  and  $\Delta C_i$  (mol L<sup>-1</sup>) are the concentration gradients of ions i and j, respectively.  $J_i$  and  $J_i$  (mol h<sup>-1</sup> m<sup>-2</sup>) are the permeation rates of ions i and j, respectively. This equation is typically used under pressure-driven conditions, whereas conductivity is commonly used for calculations under an electric field. However, these two equations are essentially the same, because flux can be converted into a product of molar concentration, fluid velocity, and the Faraday constant. Under most current test conditions, a one-to-one ion ratio has been selected to estimate the ion selectivity of the nanochannels but the concentrations of the feeding solution vary, typically ranging from 0.1 to 1 M. Altering the concentration of the feed solution can significantly impact the ion selectivity of the nanochannels, as the ion concentration influences the ion competition in nanochannels. This has led to the current evaluation of the ion selectivity in nanochannels being insufficiently comprehensive. Here, we urge researchers to systematically evaluate the ion selectivity at different feed concentrations, particularly at low ratio of target ion concentration to interfering ion concentration, to reflect a more comprehensive ion selectivity profile of the nanochannels. For instance, in evaluating Li<sup>+</sup>/Mg<sup>2+</sup> selectivity, four levels for Li<sup>+</sup>/Mg<sup>2+</sup> concentration ratio including ultralow (0.001), low (0.01), medium (0.1), and high (1) levels can

For osmotic energy harvesting, although the NaCl solution is widely accepted, other solutions such as KCl and CaCl<sub>2</sub> are also used to study the performance. It is still recommended to use a

50-fold concentration gradient (0.5 M/0.01 M) of NaCl solution as a baseline for performance evaluation due to its universal relevance. In addition, we emphasize the importance of voltage calibration as it directly affects the calculation of maximum power density, while it is easily overlooked in some studies. The equation of calculating the maximum power density ( $P_{max}$ ) is as follows:

$$P_{\text{max}} = IR_{\text{I}}^{2} \tag{2}$$

where I and  $R_{\rm L}$  are the measured diffusion current and electric load resistance, respectively. The power density reaches the maximum value when  $R_{\rm L}$  equals to the internal resistance of the membrane system ( $R_{\rm m}$ ). The  $R_{\rm m}$  can be calculated by:

$$R_{\rm m} = \frac{V_{\rm oc} - V_{\rm e}}{I} \tag{3}$$

where  $V_{\rm oc}$  is the measured open circuit voltage,  $V_{\rm e}$  is the voltage difference between two reference electrodes (Ag/AgCl) in two salt solutions with different concentrations. The voltage difference  $V_{\rm e}$  cannot be overlooked as the value could reach tens of millivolts. Therefore, it is essential to use non-ion-selective porous silicon wafers or polymer membranes for rigorous calibration to eliminate the influence of electrode potential differences at each concentration gradient.

For evaporative energy harvesting, it is necessary to conduct long-term evaluations of performance for water induced electricity generation. Temperature and humidity are two fundamental and crucial environmental factors that directly influence water evaporation, which are also easy to be monitored. Room temperature (25 °C) has been regarded as the standard temperature for test but there is no standard for humidity. Most current studies only provide the open circuit voltage or short circuit current of the device at a specific humidity level, without offering a potential or current trend across a range of varying humidity levels. The possible reason is that the relative humidity of overall environment is not easily adjustable during testing. However, it does not prevent us from controlling the humidity within a small space and monitoring its continuous impact on performance. This has practical significance because outdoor humidity can vary significantly between day and night in some regions. Therefore, in order to comprehensively and accurately evaluate the performances in evaporative energy harvesting, it may be beneficial to incorporate voltage curves related to humidity changes into the specific performance evaluation system. As for other factors affecting evaporation, such as wind speed and light, they should be considered as separate variables for study to understand their respective influence patterns.

## 5.3. High Throughput Manufacturing Methods for Framework Material Membranes and Application Expansion

Developing high throughput manufacturing methods for desired framework material membranes is a key step to industrialization of ion extraction and energy harvesting. It is dispensable to scale up the targeted framework material membranes for large-area and mass production and ultimately integrate it into a system. There are three potential development directions for

15214095, 0, Downloaded from https://advanced.onlinelibrary.wiley.com/doi/10.1002/adma.202501881 by HONG KONG POLYTECHNIC UNIVERSITY HU NG HOM, Wiley Online Library on [2609/2025]. See the Terms and Conditions (https://onlinelibrary.wiley.

om/terms-and-conditions) on Wiley Online Library for rules of use; OA articles are governed by the applicable Creative Commons

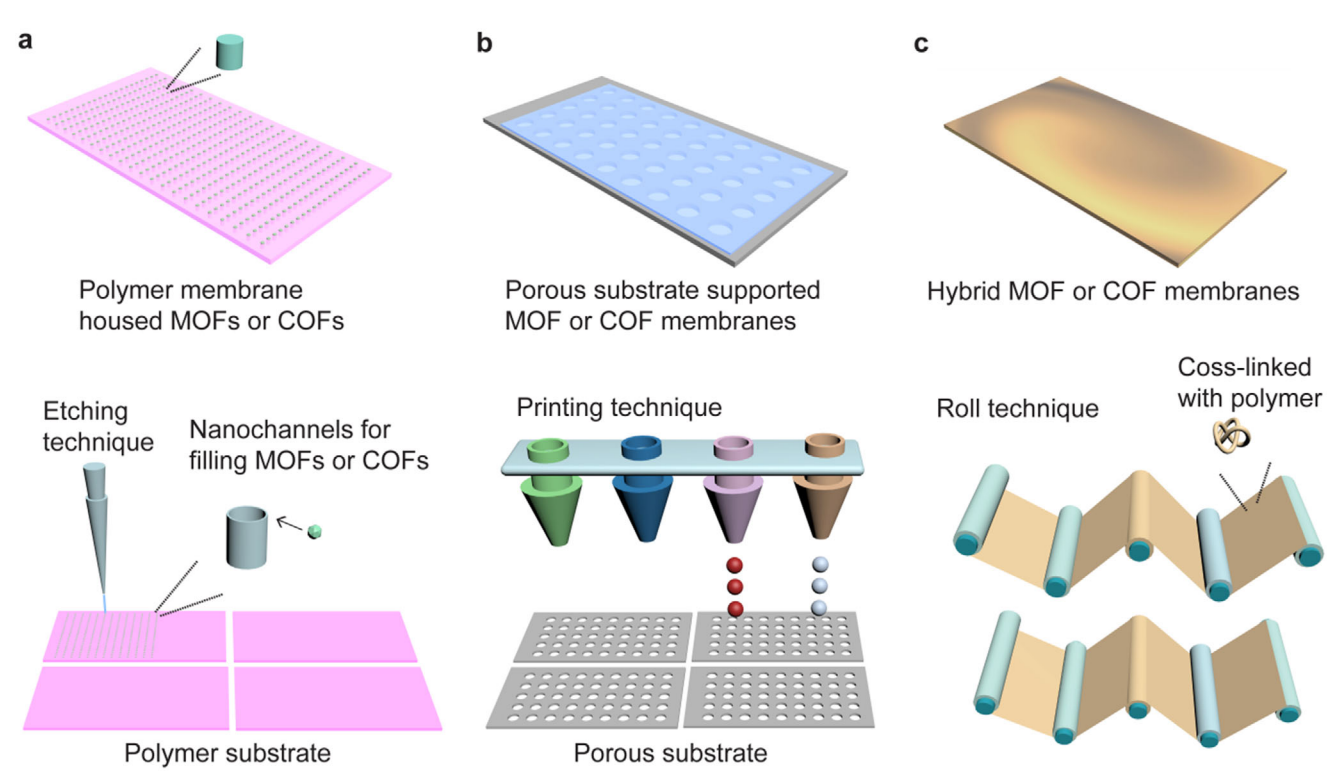


Figure 9. Three types of membranes based on framework materials are fabricated by high-throughput manufacturing methods. a) Polymer membrane housed MOFs or COFs produced through etching and filling technique. b) Porous substrate-supported MOF or COF membranes manufactured by printing technique. c) Hybrid MOF or COF membranes manufactured via roll-to-roll technique.

high-throughput manufacturing methods of framework material membranes in the future. The first one is developing etching and highly efficient growth or filling techniques to achieve the oriented assembly of MOF or COF crystals within the numerous nanopores of large-area polymer membranes (Figure 9a). The second one is developing the printing techniques to construct large-area MOF or COF membranes on the targeted robust and porous substrate (Figure 9b). The third one is advancing the rollto-roll technology to fabricate freestanding hybrid framework material membranes with interconnected structures (Figure 9c). It must be acknowledged that all three technologies present significant technical challenges in the precise synthesis of framework material membranes over large area. The primary challenge lies in the difficulty of maintaining uniformity and consistent structural orientation of framework materials during largescale growth. Specifically, surface defects in substrate, inhomogeneous contact between the solution and substrate, and evaporation of solution can all lead to issues such as non-uniform thickness, random distribution and structural orientation, cracking, and other structural defects in the large-area framework materials. Thus precise control of the substrate interface, solvent behavior, volatilization kinetics and other factors need to be conducted in resolving the challenge of structural non-uniformity in framework materials during large-area growth for the development of these three manufacturing technologies. Moreover, the cost of raw materials cannot be ignored. In high-throughput manufacturing, both the ligand quantities for MOFs and the monomer quantities for COFs can reach kilogram-scale or even higher levels. This implies that the raw material costs for both framework materials in high throughput manufacturing remain relatively high, approximately ranging from tens to hundreds of dollars per kilogram. In contrast, the production cost of MOFs at the same scale is generally higher than that of COFs due to the requirement for high-purity metal salts in the synthesis of MOFs. Optimization of ligand and monomer synthesis processes and development of recycling technologies for framework materials could offer a dual strategy to minimize raw material waste and further lower the cost.

At this stage, the roll-to-roll manufacturing method for hybrid framework materials membranes appears to be the most rapidly developing technique. In 2024, a super large-area MOFpolymer membrane with length, width and thickness of 35 m, 0.33 m, and 25 nm, respectively, has been successfully manufactured by the roll-to-roll method. [152] Such MOF hybrid membrane shows excellent and stable desalination performance exceeding thirty days in aqueous solution. More importantly, such roll-toroll method is compatible with multiple MOFs. From the current trend, the roll-to-roll method demonstrates more prominent advantages in large-area and mass production of uniform hybrid membranes, temporarily holding the leading position in high throughput manufacturing methods. In terms of membrane structure types, membranes achieved through etching and filling methods are only suitable for targeted ion extraction, whereas the substrate-supported or hybrid membranes are applicable to the osmotic or evaporative energy harvesting. Remarkably, the only current method to significantly amplify the osmotic and

15214095, 0, Downloaded from https://advanced.onlinelibrary.wiley.com/doi/10.1002/adma.202501881 by HONG KONG POLYTECHNIC UNIVERSITY HU NG HOM, Wiley Online Library on [26092025]. See the Terms and Conditions (https://onlinelibrary.wiley.com/doi/10.1002/adma.202501881 by HONG KONG POLYTECHNIC UNIVERSITY HU NG HOM, Wiley Online Library on [26092025]. See the Terms and Conditions (https://onlinelibrary.wiley.com/doi/10.1002/adma.202501881 by HONG KONG POLYTECHNIC UNIVERSITY HU NG HOM, Wiley Online Library on [26092025]. See the Terms and Conditions (https://onlinelibrary.wiley.com/doi/10.1002/adma.202501881 by HONG KONG POLYTECHNIC UNIVERSITY HU NG HOM, Wiley Online Library on [26092025]. See the Terms and Conditions (https://onlinelibrary.wiley.com/doi/10.1002/adma.202501881 by HONG KONG POLYTECHNIC UNIVERSITY HU NG HOM, Wiley Online Library on [26092025]. See the Terms and Conditions (https://onlinelibrary.wiley.com/doi/10.1002/adma.202501881 by HONG KONG POLYTECHNIC UNIVERSITY HU NG HOM, Wiley Online Library on [26092025]. See the Terms and Conditions (https://onlinelibrary.wiley.com/doi/10.1002/adma.202501881 by HONG KONG POLYTECHNIC UNIVERSITY HU NG HOM, Wiley Online Library on [26092025]. See the Terms and Conditions (https://onlinelibrary.wiley.com/doi/10.1002/adma.202501881 by HONG KONG POLYTECHNIC UNIVERSITY HU NG HOM, Wiley Online Library on [26092025]. See the Terms and Conditions (https://onlinelibrary.wiley.com/doi/10.1002/adma.202501881 by HONG KONG POLYTECHNIC UNIVERSITY HU NG HOM, Wiley Online Library on [26092025]. See the Terms and Conditions (https://onlinelibrary.wiley.com/doi/10.1002/adma.202501881 by HONG KONG POLYTECHNIC UNIVERSITY HU NG HOM, Wiley Online Library on [26092025]. See the Terms and Conditions (https://onlinelibrary.wiley.com/doi/10.1002/adma.202501881 by HONG KONG POLYTECHNIC UNIVERSITY HU NG HOM, Wiley Online Library on [26092025]. See the Terms and Conditions (https://onlinelibrary.wiley.com/doi/10.1002/adma.202501881 by HONG KONG POLYTECHNIC UNIVERSITY HU NG HOM POLYTECHNIC

convierms- and-conditions) on Wiley Online Library for rules of use; OA articles are governed by the applicable Creative Commons L

www.advancedsciencenews.com

ADVANCED MATERIALS

evaporative power generation performance is to connect a large number of small devices in series and parallel. However, the energy harvesting performance of the ultimately scaled-up framework material membranes in series and parallel connection must be reassessed due to uncertainties like defects in framework materials that may arise during the scaling process. Additionally, the impact of actual environmental conditions such as humidity, temperature, and water salinity cannot be ignored because the performances of large-scale assembled devices may be severely affected under these complex and variable environmental conditions. From these perspectives, high throughput manufacturing methods for framework material membranes needs ongoing feedback from comprehensive performance evaluations to achieve refinement.

Besides, a deep study on nanofluidics and high throughput manufacturing methods for MOFs and COFs would also drive the development of other fluid and membrane-related sciences and technologies, such as seawater desalination. A representative example in MOF membrane based desalination is that the polyamide incorporated with amphiphilic Cu-MOFs could act as a reverse osmosis membrane for rejection of salt, boron and N-nitrosodimethylamine.[153] In the future, other high-performance membranes based on framework materials are expected to be designed to filter other pollutants in brackish water and seawater, which further increase the existing freshwater supply. In this regard, careful consideration of many features in framework materials needs to be required, including suitable pore sizes, tolerance to high-salt and high-pressure environment, as well as the anti-fouling capabilities. On the other hand, an intriguing vision is to develop an integrated system combining seawater desalination, evaporative energy generation, and electrodialysis. In this system, desalinated water would be used for direct evaporation to generate electricity, which would then be stored and utilized for ions sieving via electrodialysis. Special attention should be given to optimizing energy efficiency within this system.

## 6. Conclusion

Overall, we attempt to construct a comprehensive picture to understand the current advancements and existing challenges in framework materials-based ion sieving and energy harvesting in the water systems. MOFs and COFs as framework materials with inherent nanochannels showcase unprecedented potential for practical applications of ion extraction including Li+ and Fions from lakes and seawater, osmotic and evaporative energy harvesting in real environment, which would enormously impact the development of human society. Fundamentally, ion-selective transport properties within the framework materials determine whether they can operate efficiently, long-term, and stably in an aqueous environment. Centered on this key behavioral characteristic, fully revealing the mechanisms of nanofluidics, optimizing existing or developing new high-performance framework materials and corresponding high-throughput manufacturing methods, and advancing integrated series-parallel models to achieve industrial-grade performance, are the focus areas for both the present and future. Through in-depth collaboration between scientists and engineers to address these issues, it would be a considerable leap to create framework materials -based smart systems on demand for matter and electricity acquisition. As an interdisciplinary field, we envision that framework material-based nanofluidics feature huge opportunities to create new watermatter-energy nexus in the future.

## Acknowledgements

M.Z. thanks for the financial support of the National Natural Science Foundation of China (62205276), the Hong Kong Research Grants Council (PolyU 15308324), the PolyU Research Center for Organic Electronics (1-CE32) and the PolyU Postdoc Matching Fund Scheme (1-W34A). W.Y.W. acknowledges the support from the RGC Senior Research Fellowship Scheme (SRFS2021-5S01), Hong Kong Research Grants Council (PolyU 15307321), Research Institute for Smart Energy (CDAQ), Research Centre for Carbon-Strategic Catalysis (CE2L and CE41) and Miss Clarea Au for the Endowed Professorship in Energy (847S). H.L. acknowledges the National Natural Science Foundation of China (52171069).

#### **Conflict of Interest**

The authors declare no conflict of interest.

#### **Keywords**

evaporative energy conversion, framework materials, ion extraction, nanofluidics, osmotic energy harvesting

Received: January 26, 2025 Revised: May 23, 2025 Published online:

- P. Mehta, S. Siebert, M. Kummu, Q. Deng, T. Ali, L. Marston, W. Xie, K. F. Davis, Nat. Water 2024, 2, 254.
- [2] Z. Wu, H. Zhai, E. J. Grol, C. M. Able, N. S. Siefert, *Nat. Water* 2023, 1, 471.
- [3] A. Tzachor, H. Wang, C. E. Richards, Nat. Water 2024, 2, 4.
- [4] M. Rastgar, K. Moradi, C. Burroughs, A. Hemmati, E. Hoek, M. Sadrzadeh, Chem. Rev. 2023, 123, 10156.
- [5] X. Chen, M. Yang, S. Zheng, F. Temprano-Coleto, Q. Dong, G. Cheng, N. Yao, H. A. Stone, L. Hu, Z. J. Ren, *Nat. Water* **2023**, *1*, 808.
- [6] W. Xu, H. Zheng, Y. Liu, X. Zhou, C. Zhang, Y. Song, X. Deng, M. Leung, Z. Yang, R. X. Xu, Z. L. Wang, X. C. Zeng, Z. Wang, *Nature* 2020, 578, 392.
- [7] L. Wang, W. Li, Y. Song, W. Xu, Y. Jin, C. Zhang, Z. Wang, Adv. Funct. Mater. 2022, 32, 2206705.
- [8] Y. Xiong, J. Zhou, P. Lu, J. Yin, Y. Wang, Z. Fan, Matter 2022, 5, 1760.
- [9] Q. Lin, L. Gong, F. Jiang, C. Deng, S. Xiang, Y. Ye, B. Chen, Coord. Chem. Rev. 2024, 515, 215971.
- [10] T. Ye, H. Gao, Q. Li, N. Liu, X. Liu, L. Jiang, J. Gao, Angew. Chem. Int. Ed. 2024, 63, 202316161.
- [11] X. Li, H. Zhang, P. Wang, J. Hou, J. Lu, C. D. Easton, X. Zhang, M. R. Hill, A. W. Thornton, J. Z. Liu, B. D. Freeman, A. J. Hill, L. Jiang, H. Wang, Nat. Commun. 2019, 10, 2490.
- [12] W. Liang, X. Zhang, L. Wang, C. Wen, L. Tian, Z. Li, X. Chen, W. Wu, Chem. Sci. 2024, 15, 10455.
- [13] Y. Zhou, L. Jiang, Joule 2020, 4, 2244.
- [14] F. La Mantia, M. Pasta, H. D. Deshazer, B. E. Logan, Y. Cui, Nano Lett. 2011, 11, 1810.
- [15] J. Tang, Y. Wang, H. Yang, Q. Zhang, C. Wang, L. Li, Z. Zheng, Y. Jin, H. Wang, Y. Gu, T. Zuo, Nat. Commun. 2024, 15, 3649.
- [16] J. Lin, W. Ye, S. Xie, J. Du, R. Liu, D. Zou, X. Chen, Z. Yu, S. Fang, E. Y. M. Ang, W. Toh, D. D. Han, T. Y. Ng, D. H. Seo, S. Zhao, B. Van der Bruggen, M. Xie, Y. M. Lee, *Nat. Water* 2023, 1, 725.



www.advmat.de

- [17] Z. Zhang, L. Wen, L. Jiang, Nat. Rev. Mater. 2021, 6, 622.
- [18] J. Wang, Z. Cui, S. Li, Z. Song, M. He, D. Huang, Y. Feng, Y. Liu, K. Zhou, X. Wang, L. Wang, Nat. Commun. 2024, 15, 608.
- [19] A.-H. Cavusoglu, X. Chen, P. Gentine, O. Sahin, Nat. Commun. 2017, 8, 617.
- [20] G. Xue, Y. Xu, T. Ding, J. Li, J. Yin, W. Fei, Y. Cao, J. Yu, L. Yuan, L. Gong, J. Chen, S. Deng, J. Zhou, W. Guo, *Nat. Nanotechnol.* 2017, 12, 317.
- [21] T. Li, M. Wu, J. Xu, R. Du, T. Yan, P. Wang, Z. Bai, R. Wang, S. Wang, Nat. Commun. 2022, 13, 6771.
- [22] J. Tan, S. Fang, Z. Zhang, J. Yin, L. Li, X. Wang, W. Guo, Nat. Commun. 2022, 13, 3643.
- [23] Q. Ma, Q. He, P. Yin, H. Cheng, X. Cui, Q. Yun, H. Zhang, Adv. Mater. 2020, 32, 2003720.
- [24] X. Wang, F. Lin, X. Wang, S. Fang, J. Tan, W. Chu, R. Rong, J. Yin, Z. Zhang, Y. Liu, W. Guo, Chem. Soc. Rev. 2022, 51, 4902.
- [25] Y. Qin, Y. Wang, X. Sun, Y. Li, H. Xu, Y. Tan, Y. Li, T. Song, B. Sun, Angew. Chem., Int. Ed. 2020, 59, 10619.
- [26] H. Zhang, X. Li, J. Hou, L. Jiang, H. Wang, Chem. Soc. Rev. 2022, 51, 2224
- [27] P. Liu, X.-Y. Kong, L. Jiang, L. Wen, Chem. Soc. Rev. 2024, 53, 2972.
- [28] L. Bocquet, Nat. Mater. 2020, 19, 254.
- [29] S. Kim, H. Choi, B. Kim, G. Lim, T. Kim, M. Lee, H. Ra, J. Yeom, M. Kim, E. Kim, J. Hwang, J. S. Lee, W. Shim, Adv. Mater. 2023, 35, 2206354.
- [30] D. Lei, Z. Zhang, L. Jiang, Chem. Soc. Rev. 2024, 53, 2300.
- [31] W. Xin, H. Ling, Y. Cui, Y. Qian, X.-Y. Kong, L. Jiang, L. Wen, J. Phys. Chem. Lett. 2023, 14, 627.
- [32] X. Yu, W. Ren, Adv. Funct. Mater. 2024, 34, 2313968.
- [33] A. Siria, P. Poncharal, A.-L. Biance, R. Fulcrand, X. Blase, S. T. Purcell, L. Bocquet, *Nature* 2013, 494, 455.
- [34] C. Chen, D. Liu, L. He, S. Qin, J. Wang, J. M. Razal, N. A. Kotov, W. Lei, *Joule* 2020, 4, 247.
- [35] Z. Xie, Z. Xiang, X. Fu, Z. Lin, C. Jiao, K. Zheng, M. Yang, X. Qin, D. Ye, ACS Energy Lett. 2024, 9, 2092.
- [36] F. H. J. van der Heyden, D. J. Bonthuis, D. Stein, C. Meyer, C. Dekker, Nano Lett. 2006, 6, 2232.
- [37] Q. Hu, X. Lin, G. Ren, J. Lü, W. Wang, D. Zhang, S. Zhou, *Nat. Water* 2024, 2, 988.
- [38] Y. Hu, W. Yang, W. Wei, Z. Sun, B. Wu, K. Li, Y. Li, Q. Zhang, R. Xiao, C. Hou, H. Wang, Sci. Adv. 2024, 10, adk4620.
- [39] S. Fang, J. Li, Y. Xu, C. Shen, W. Guo, Joule 2022, 6, 690.
- [40] A. Esfandiar, B. Radha, F. C. Wang, Q. Yang, S. Hu, S. Garaj, R. R. Nair, A. K. Geim, K. Gopinadhan, Science 2017, 358, 511.
- [41] Y. Jiang, R. Hu, C. Yang, Z. Zhou, G. Yuan, H. Zhou, S. Hu, Sci. Adv. 2023, 9, adi8493.
- [42] J. Wang, Z. Zhang, J. Zhu, M. Tian, S. Zheng, F. Wang, X. Wang, L. Wang, Nat. Commun. 2020, 11, 3540.
- [43] L. Ding, M. Zheng, D. Xiao, Z. Zhao, J. Xue, S. Zhang, J. Caro, H. Wang, Angew. Chem., Int. Ed. 2022, 61, 202206152.
- [44] B. Luan, R. Zhou, Nano Lett. 2019, 19, 977.
- [45] J. Feng, K. Liu, M. Graf, D. Dumcenco, A. Kis, M. Di Ventra, A. Radenovic, Nat. Mater. 2016, 15, 850.
- [46] J. Feng, M. Graf, K. Liu, D. Ovchinnikov, D. Dumcenco, M. Heiranian, V. Nandigana, N. R. Aluru, A. Kis, A. Radenovic, *Nature* 2016, 536, 197.
- [47] J. Safaei, Y. Gao, M. Hosseinpour, X. Zhang, Y. Sun, X. Tang, Z. Zhang, S. Wang, X. Guo, Y. Wang, Z. Chen, D. Zhou, F. Kang, L. Jiang, G. Wang, J. Am. Chem. Soc. 2023, 145, 2669.
- [48] Z. Zhang, P. Bhauriyal, H. Sahabudeen, Z. Wang, X. Liu, M. Hambsch, S. C. B. Mannsfeld, R. Dong, T. Heine, X. Feng, Nat. Commun. 2022, 13, 3935.
- [49] J. Lu, H. Zhang, J. Hou, X. Li, X. Hu, Y. Hu, C. D. Easton, Q. Li, C. Sun, A. W. Thornton, M. R. Hill, X. Zhang, G. Jiang, J. Z. Liu,

- A. J. Hill, B. D. Freeman, L. Jiang, H. Wang, Nat. Mater. 2020, 19, 767.
- [50] F. Sheng, B. Wu, X. Li, T. Xu, M. A. Shehzad, X. Wang, L. Ge, H. Wang, T. Xu, Adv. Mater. 2021, 33, 2104404.
- [51] J. Lu, H. Wang, Matter 2021, 4, 2810.
- [52] J. Lu, X. Hu, K. M. Ung, Y. Zhu, X. Zhang, H. Wang, Acc. Mater. Res. 2022, 3, 735.
- [53] M. D. Allendorf, R. Dong, X. Feng, S. Kaskel, D. Matoga, V. Stavila, Chem. Rev. 2020, 120, 8581.
- [54] R. Freund, O. Zaremba, G. Arnauts, R. Ameloot, G. Skorupskii, M. Dincă, A. Bavykina, J. Gascon, A. Ejsmont, J. Goscianska, M. Kalmutzki, U. Lächelt, E. Ploetz, C. S. Diercks, S. Wuttke, Angew. Chem., Int. Ed. 2021, 60, 23975.
- [55] R.-B. Lin, B. Chen, Chem 2022, 8, 2114.
- [56] Z. Zhang, Y. Ye, S. Xiang, B. Chen, Acc. Chem. Res. 2022, 55, 3752.
- [57] Y. Tian, F. Cui, Z. Bian, X. Tao, H. Wang, N. Zhang, G. Zhu, Acc. Chem. Res. 2024, 57, 2130.
- [58] G. Xing, D. Peng, T. Ben, Chem. Soc. Rev. 2024, 53, 1495.
- [59] Y. Fang, Y. Liu, L. Qi, Y. Xue, Y. Li, Chem. Soc. Rev. 2022, 51, 2681.
- [60] H. Wang, Y. Zhang, J. Wang, Saijilahu, H. S, H. Yang, X.-H. Xia, C. Wang, Adv. Funct. Mater. 2025, 35, 2412477.
- [61] C. I. Lynch, S. Rao, M. S. P. Sansom, Chem. Rev. 2020, 120, 10298.
- [62] S. Goutham, A. Keerthi, A. Ismail, A. Bhardwaj, H. Jalali, Y. You, Y. Li, N. Hassani, H. Peng, M. V. S. Martins, F. Wang, M. Neek-Amal, B. Radha, Nat. Nanotechnol. 2023, 18, 596.
- [63] C. Lu, C. Hu, C. L. Ritt, X. Hua, J. Sun, H. Xia, Y. Liu, D.-W. Li, B. Ma, M. Elimelech, J. Qu, J. Am. Chem. Soc. 2021, 143, 14242.
- [64] R. Epsztein, R. M. DuChanois, C. L. Ritt, A. Noy, M. Elimelech, Nat. Nanotechnol. 2020, 15, 426.
- [65] Y. Guo, Y. Ying, Y. Mao, X. Peng, B. Chen, Angew. Chem., Int. Ed. 2016, 55, 15120.
- [66] H. Zhang, J. Hou, Y. Hu, P. Wang, R. Ou, L. Jiang, J. Z. Liu, B. D. Freeman, A. J. Hill, H. Wang, Sci. Adv. 2018, 4, aaq0066.
- [67] J. Lu, H. Zhang, X. Hu, B. Qian, J. Hou, L. Han, Y. Zhu, C. Sun, L. Jiang, H. Wang, ACS Nano 2021, 15, 1240.
- [68] J. Lu, H. Xu, H. Yu, X. Hu, J. Xia, Y. Zhu, F. Wang, H.-A. Wu, L. Jiang, H. Wang, Sci. Adv. 2022, 8, abl5070.
- [69] X. Li, G. Jiang, M. Jian, C. Zhao, J. Hou, A. W. Thornton, X. Zhang, J. Z. Liu, B. D. Freeman, H. Wang, L. Jiang, H. Zhang, Nat. Commun. 2023, 14, 286.
- [70] G. Laucirica, J. A. Allegretto, M. F. Wagner, M. E. Toimil-Molares, C. Trautmann, M. Rafti, W. Marmisollé, O. Azzaroni, Adv. Mater. 2022, 34, 2207339.
- [71] H. Zhou, T. Tang, R. Hu, Y. Jiang, G. Yuan, H. Wang, C. Wang, S. Hu, Nano Lett. 2024, 24, 6296.
- [72] Q. Zhang, P.-S. Cao, Y. Cheng, S.-S. Yang, Y.-D. Yin, T.-Y. Lv, Z.-Y. Gu, Adv. Funct. Mater. 2020, 30, 2004854.
- [73] R.-J. Mo, S. Chen, L.-Q. Huang, X.-L. Ding, S. Rafique, X.-H. Xia, Z.-O. Li, *Nat. Commun.* 2024, 15, 2145.
- [74] J. Lu, G. Jiang, H. Zhang, B. Qian, H. Zhu, Q. Gu, Y. Yan, J. Z. Liu, B. D. Freeman, L. Jiang, H. Wang, Sci. Adv. 2023, 9, abq1369.
- [75] J. Hou, H. Zhang, A. W. Thornton, A. J. Hill, H. Wang, K. Konstas, Adv. Funct. Mater. 2021, 31, 2105991.
- [76] R. Xu, Y. Kang, W. Zhang, X. Zhang, B. Pan, Angew. Chem., Int. Ed. 2022, 61, 202115443.
- [77] H. Xiao, M. Chai, A. Hosseini, A. H. Korayem, M. Abdollahzadeh, H. Ahmadi, V. Chen, D. B. Gore, M. Asadnia, A. Razmjou, J. Membr. Sci. 2023, 670, 121312.
- [78] C. Zhao, F. Feng, J. Hou, J. Hu, Y. Su, J. Z. Liu, M. Hill, B. D. Freeman, H. Wang, H. Zhang, J. Am. Chem. Soc. 2024, 146, 14058.
- [79] M. Abdollahzadeh, M. Chai, E. Hosseini, M. Zakertabrizi, M. Mohammad, H. Ahmadi, J. Hou, S. Lim, A. Habibnejad Korayem, V. Chen, M. Asadnia, A. Razmjou, Adv. Mater. 2022, 34, 2107878.



www.advmat.de

- [80] J. Li, Y. Shi, C. Qi, B. Zhang, X. Xing, Y. Li, T. Chen, X. Mao, Z. Zuo, X. Zhao, Z. Pan, L. Li, X. Yang, C. Li, Angew. Chem., Int. Ed. 2023, 62, 202309918.
- [81] X. Wu, H. Zhang, X. Zhang, Q. Guan, X. Tang, H. Wu, M. Feng, H. Wang, R. Ou, Proc. Natl. Acad. Sci. 2024, 121, 2309852121.
- [82] M. Chen, T. Liu, X. Zhang, R. Zhang, S. Tang, Y. Yuan, Z. Xie, Y. Liu, H. Wang, K. V. Fedorovich, N. Wang, Adv. Funct. Mater. 2021, 31, 2100106.
- [83] Y. Peng, H. Huang, Y. Zhang, C. Kang, S. Chen, L. Song, D. Liu, C. Zhong, Nat. Commun. 2018, 9, 187.
- [84] Y. Yuan, S. Feng, L. Feng, Q. Yu, T. Liu, N. Wang, Angew. Chem. Int. Ed. 2020, 59, 4262.
- [85] L. N. McHugh, M. J. McPherson, L. J. McCormick, S. A. Morris, P. S. Wheatley, S. J. Teat, D. McKay, D. M. Dawson, C. E. F. Sansome, S. E. Ashbrook, C. A. Stone, M. W. Smith, R. E. Morris, *Nat. Chem.* 2018, 10, 1096.
- [86] J. A. Allegretto, G. Laucirica, A. L. Huamani, M. F. Wagner, A. G. Albesa, M. E. Toimil-Molares, M. Rafti, W. Marmisollé, O. Azzaroni, ACS Nano 2024, 18, 18572.
- [87] A. L. Huamani, G. Laucirica, J. A. Allegretto, M. E. Toimil-Molares, A. S. Picco, M. R. Ceolín, A. R. Passos, O. Azzaroni, W. A. Mamisollé, M. Rafti, *Inorg. Chem. Front.* 2024, 11, 8627.
- [88] H. Wang, Z. Zeng, P. Xu, L. Li, G. Zeng, R. Xiao, Z. Tang, D. Huang, L. Tang, C. Lai, D. Jiang, Y. Liu, H. Yi, L. Qin, S. Ye, X. Ren, W. Tang, *Chem. Soc. Rev.* 2019, 48, 488.
- [89] S. Bing, W. Xian, S. Chen, Y. Song, L. Hou, X. Liu, S. Ma, Q. Sun, L. Zhang, Matter 2021, 4, 2027.
- [90] H. Wang, Y. Zhai, Y. Li, Y. Cao, B. Shi, R. Li, Z. Zhu, H. Jiang, Z. Guo, M. Wang, L. Chen, Y. Liu, K.-G. Zhou, F. Pan, Z. Jiang, *Nat. Commun.* 2022, 13, 7123.
- [91] L. Cao, I. C. Chen, Z. Li, X. Liu, M. Mubashir, R. A. Nuaimi, Z. Lai, Nat. Commun. 2022, 13, 7894.
- [92] T. Wu, Y. Qian, Z. Zhu, W. Yu, L. Zhang, J. Liu, X. Shen, X. Zhou, T. Qian, C. Yan, Adv. Mater. 2025, 37, 2415509.
- [93] W. Meng, S. Chen, Z. Guo, F. Gao, J. Wang, J. Lu, Y. Hou, Q. He, X. Zhan, M. Qiu, Q. Zhang, Nat. Water 2025, 3, 191.
- [94] B. Lyu, M. Wang, J. Jiang, Z. Jiang, J. Membr. Sci. 2022, 662, 120976.
- [95] Q.-W. Meng, X. Zhu, W. Xian, S. Wang, Z. Zhang, L. Zheng, Z. Dai, H. Yin, S. Ma, Q. Sun, Proc. Natl. Acad. Sci. 2024, 121, 2316716121.
- [96] M. Wang, P. Zhang, X. Liang, J. Zhao, Y. Liu, Y. Cao, H. Wang, Y. Chen, Z. Zhang, F. Pan, Z. Zhang, Z. Jiang, Nat. Sustain. 2022, 5, 518.
- [97] S. Zhao, C. Jiang, J. Fan, S. Hong, P. Mei, R. Yao, Y. Liu, S. Zhang, H. Li, H. Zhang, C. Sun, Z. Guo, P. Shao, Y. Zhu, J. Zhang, L. Guo, Y. Ma, J. Zhang, X. Feng, F. Wang, H. Wu, B. Wang, *Nat. Mater.* 2021, 20, 1551.
- [98] Y. Pan, H. Liu, Z. Huang, W. Zhang, H. Gao, L. Liang, L. Dong, H. Meng, Angew. Chem., Int. Ed. 2024, 63, 202316315.
- [99] X. Li, Y. Mo, W. Qing, S. Shao, C. Y. Tang, J. Li, J. Membr. Sci. 2019, 591, 117317.
- [100] Y. Zhao, T. Tong, X. Wang, S. Lin, E. M. Reid, Y. Chen, *Environ. Sci. Technol.* 2021, 55, 1359.
- [101] X.-Y. Nie, S.-Y. Sun, X. Song, J.-G. Yu, J. Membr. Sci. 2017, 530, 185.
- [102] Z.-y. Ji, Q.-b. Chen, J.-s. Yuan, J. Liu, Y.-y. Zhao, W.-x. Feng, Sep. Purif. Technol. 2017, 172, 168.
- [103] R. Li, J. Jiang, Q. Liu, Z. Xie, J. Zhai, Nano Energy 2018, 53, 643.
- [104] C. Wang, F.-F. Liu, Z. Tan, Y.-M. Chen, W.-C. Hu, X.-H. Xia, Adv. Funct. Mater. 2020, 30, 1908804.
- [105] Y.-C. Liu, L.-H. Yeh, M.-J. Zheng, K. C.-W. Wu, Sci. Adv. 2021, 7, abe9924.
- [106] J. Xiao, M. Cong, M. Li, X. Zhang, Y. Zhang, X. Zhao, W. Lu, Z. Guo, X. Liang, G. Qing, Adv. Funct. Mater. 2024, 34, 2307996.

- [107] R. K. Tonnah, M. Chai, M. Abdollahzadeh, H. Xiao, M. Mohammad, E. Hosseini, M. Zakertabrizi, D. Jarrahbashi, A. Asadi, A. Razmjou, M. Asadnia, ACS Nano 2023, 17, 12445.
- [108] S. Pan, P. Liu, Q. Li, B. Zhu, X. Liu, J. Lao, J. Gao, L. Jiang, Angew. Chem., Int. Ed. 2023, 62, 202218129.
- [109] Z.-J. Yang, L.-H. Yeh, Y.-H. Peng, Y.-P. Chuang, K. C.-W. Wu, Angew. Chem., Int. Ed. 2024, 63, 202408375.
- [110] L. Liu, Z. Chen, J. Wang, D. Zhang, Y. Zhu, S. Ling, K.-W. Huang, Y. Belmabkhout, K. Adil, Y. Zhang, B. Slater, M. Eddaoudi, Y. Han, Nat. Chem. 2019, 11, 622.
- [111] C. Chen, L. Meng, L. Cao, D. Zhang, S. An, L. Liu, J. Wang, G. Li, T. Pan, J. Shen, Z. Chen, Z. Shi, Z. Lai, Y. Han, J. Am. Chem. Soc. 2024, 146, 11855.
- [112] J. D. Hem, US Geological Survey 1985, 2254, 1.
- [113] Q. Li, K. Zhou, B. Zhu, X. Liu, J. Lao, J. Gao, L. Jiang, J. Am. Chem. Soc. 2023, 145, 28038.
- [114] Z.-Q. Li, G.-L. Zhu, R.-J. Mo, M.-Y. Wu, X.-L. Ding, L.-Q. Huang, Z.-Q. Wu, X.-H. Xia, Angew. Chem., Int. Ed. 2022, 61, 202202698.
- [115] J. Wang, Z. Song, M. He, Y. Qian, D. Wang, Z. Cui, Y. Feng, S. Li, B. Huang, X. Kong, J. Han, L. Wang, Nat. Commun. 2024, 15, 2125.
- [116] C. Wang, J. Tang, L. Li, J. Wan, Y. Ma, Y. Jin, J. Liu, H. Wang, Q. Zhang, Adv. Funct. Mater. 2022, 32, 2204068.
- [117] L. Cao, I. C. Chen, X. Liu, Z. Li, Z. Zhou, Z. Lai, ACS Nano 2022, 16, 18910.
- [118] L. Cao, I. C. Chen, C. Chen, D. B. Shinde, X. Liu, Z. Li, Z. Zhou, Y. Zhang, Y. Han, Z. Lai, J. Am. Chem. Soc. 2022, 144, 12400.
- [119] J. Yang, B. Tu, G. Zhang, P. Liu, K. Hu, J. Wang, Z. Yan, Z. Huang, M. Fang, J. Hou, Q. Fang, X. Qiu, L. Li, Z. Tang, *Nat. Nanotechnol.* 2022, 17, 622.
- [120] X. Shi, Z. Zhang, S. Fang, J. Wang, Y. Zhang, Y. Wang, Nano Lett. 2021, 21, 8355.
- [121] X. Shi, Z. Zhang, M. Wei, X. Wang, J. Wang, Y. Zhang, Y. Wang, *Macro-molecules* 2022, 55, 3259.
- [122] T. Zhu, Y. Kong, B. Lyu, L. Cao, B. Shi, X. Wang, X. Pang, C. Fan, C. Yang, H. Wu, Z. Jiang, Nat. Commun. 2023, 14, 5926.
- [123] Q. Guo, Z. Lai, X. Zuo, W. Xian, S. Wu, L. Zheng, Z. Dai, S. Wang, Q. Sun, Nat. Commun. 2023, 14, 6702.
- [124] W. Jiang, J. Zhou, X. Zhong, M. Fang, J. Hao, D. Zhao, X. Wen, H. Wang, Y. Zhou, Y. Zhu, L. Jiang, Nat. Sustain. 2025, 8, 446.
- [125] T. Thorsen, T. Holt, J. Membr. Sci. 2009, 335, 103.
- [126] X. Ma, Z. Li, Z. Deng, D. Chen, X. Wang, X. Wan, Z. Fang, X. Peng, J. Mater. Chem. A 2021, 9, 9048.
- [127] Z. Li, X. Ma, D. Chen, X. Wan, X. Wang, Z. Fang, X. Peng, Adv. Sci. 2021, 8, 2004552.
- [128] Z. Wang, Y. Wu, K. Xu, L. Jiang, J. Sun, G. Cai, G. Li, B. Y. Xia, H. Liu, Adv. Funct. Mater. 2021, 31, 2104732.
- [129] H. Liu, P. Cui, J. Zhang, J. Wang, Y. Ge, Z. Zhou, Y. Meng, Z. Huang, K. Yang, Z. Du, G. Cheng, Small 2024, 20, 2400961.
- [130] Z. Wang, Y. Huang, T. Zhang, K. Xu, X. Liu, A. Zhang, Y. Xu, X. Zhou, J. Dai, Z. Jiang, G. Zhang, H. Liu, B. Y. Xia, J. Am. Chem. Soc. 2024, 146, 1690.
- [131] M. Liu, C. Shang, T. Zhao, H. Yu, Y. Kou, Z. Lv, M. Hou, F. Zhang, Q. Li, D. Zhao, X. Li, Nat. Commun. 2023, 14, 1211.
- [132] Y. Zhao, L. Zhu, Y. Kang, C.-H. Shen, X. Liu, D. Jiang, L. Fu, O. Guselnikova, L. Huang, X. Song, T. Asahi, Y. Yamauchi, ACS Nano 2024, 18, 22404.
- [133] M. Liu, Z. Lv, Y. Peng, Y. Kou, T. Zhao, H. Yu, J. Jia, L. Gao, C. Shang, F. Zhang, D. Zhao, X. Li, Angew. Chem. Int. Ed. 2025, 64, 202423939.
- [134] Z. Lv, R. Lin, Y. Yang, K. Lan, C.-T. Hung, P. Zhang, J. Wang, W. Zhou, Z. Zhao, Z. Wang, J. Zou, T. Wang, T. Zhao, Y. Xu, D. Chao, W. Tan, B. Yan, Q. Li, D. Zhao, X. Li, *Nat. Chem.* 2025, 17, 177
- [135] R. Saini, A. Garg, D. P. J. Barz, Langmuir 2014, 30, 10950.
- [136] E. R. Nightingale, Jr., J. Phys. Chem. 1959, 63, 1381.

and Conditions (https://onlinelibrary.wiley.

com/terms-and-conditions) on Wiley Online Library for rules of use; OA articles are governed by the applicable Creative Commons



www.advmat.de

- [137] S. Faucher, N. Aluru, M. Z. Bazant, D. Blankschtein, A. H. Brozena, J. Cumings, J. Pedro de Souza, M. Elimelech, R. Epsztein, J. T. Fourkas, A. G. Rajan, H. J. Kulik, A. Levy, A. Majumdar, C. Martin, M. McEldrew, R. P. Misra, A. Noy, T. A. Pham, M. Reed, E. Schwegler, Z. Siwy, Y. Wang, M. Strano, J. Phys. Chem. C 2019, 123, 21309.
- [138] J. E. Mondloch, M. J. Katz, N. Planas, D. Semrouni, L. Gagliardi, J. T. Hupp, O. K. Farha, Chem. Commun. 2014, 50, 8944.
- [139] C. Prehal, D. Weingarth, E. Perre, R. T. Lechner, H. Amenitsch, O. Paris, V. Presser, Energy Environ. Sci. 2015, 8, 1725.
- [140] C. Prehal, C. Koczwara, N. Jäckel, A. Schreiber, M. Burian, H. Amenitsch, M. A. Hartmann, V. Presser, O. Paris, *Nat. Energy* 2017, 2 16215
- [141] M. Favaro, B. Jeong, P. N. Ross, J. Yano, Z. Hussain, Z. Liu, E. J. Crumlin, Nat. Commun. 2016, 7, 12695.
- [142] K. V. Agrawal, S. Shimizu, L. W. Drahushuk, D. Kilcoyne, M. S. Strano, Nat. Nanotechnol. 2017, 12, 267.
- [143] Z. Chen, C. Hu, C. Lu, J. Sun, Y. Zhang, F. Wang, J. Qu, ACS Nano 2023, 17, 12629.
- [144] C. Lu, C. Hu, Z. Chen, P. Wang, F. Feng, G. He, F. Wang, Y. Zhang, J. Z. Liu, X. Zhang, J. Qu, Sci. Adv. 2023, 9, adf8412.
- [145] P. Zelenovskii, M. Soares, C. Bornes, I. Marin-Montesinos, M. Sardo, S. Kopyl, A. Kholkin, L. Mafra, F. Figueiredo, *Nat. Commun.* 2024, 15, 5516.

- [146] L. K. S. Bonagiri, K. S. Panse, S. Zhou, H. Wu, N. R. Aluru, Y. Zhang, ACS Nano 2022, 16, 19594.
- [147] N. R. Aluru, F. Aydin, M. Z. Bazant, D. Blankschtein, A. H. Brozena, J. P. de Souza, M. Elimelech, S. Faucher, J. T. Fourkas, V. B. Koman, M. Kuehne, H. J. Kulik, H.-K. Li, Y. Li, Z. Li, A. Majumdar, J. Martis, R. P. Misra, A. Noy, T. A. Pham, H. Qu, A. Rayabharam, M. A. Reed, C. L. Ritt, E. Schwegler, Z. Siwy, M. S. Strano, Y. Wang, Y.-C. Yao, C. Zhan, et al., Chem. Rev. 2023, 123, 2737.
- [148] L. Fumagalli, A. Esfandiar, R. Fabregas, S. Hu, P. Ares, A. Janardanan, Q. Yang, B. Radha, T. Taniguchi, K. Watanabe, G. Gomila, K. S. Novoselov, A. K. Geim, *Science* 2018, 360, 1339.
- [149] R. Zhou, M. Neek-Amal, F. M. Peeters, B. Bai, C. Sun, Phys. Rev. Lett. 2024, 132, 184001.
- [150] Y. Li, Z. Li, R. P. Misra, C. Liang, A. J. Gillen, S. Zhao, J. Abdullah, T. Laurence, J. A. Fagan, N. Aluru, D. Blankschtein, A. Noy, *Nat. Mater.* 2024, 23, 1123.
- [151] N. Kavokine, Nat. Nanotechnol. 2023, 18, 102.
- [152] Y.-L. Ji, B.-X. Gu, H.-Q. Huo, S.-J. Xie, H. Peng, W.-H. Zhang, M.-J. Yin, B. Xiong, H. Lu, L. F. Villalobos, Q. Zhao, C.-J. Gao, M. Elimelech, Q.-F. An, *Nat. Water* **2024**, *2*, 183.
- [153] Y. Wen, R. Dai, X. Li, X. Zhang, X. Cao, Z. Wu, S. Lin, C. Y. Tang, Z. Wang, Sci. Adv. 2022, 8, abm4149.



**Zhengyun Wang** received his Ph.D. degree from Huazhong University of Science and Technology in 2020. After postdoctoral work at Huazhong University of Science and Technology from 2020 to 2024, he then carried out postdoctoral research in the Department of Applied Biology and Chemical Technology at the Hong Kong Polytechnic University in 2024. His research interests focus on framework materials synthesis and specificity-related application technology including sensing and energy conversion.



**Miao Zhang** received her Ph.D. degree from Beijing Jiaotong University. She then carried out postdoctoral research through the Hong Kong Scholars Program from 2019 to 2021 in the Department of Applied Biology and Chemical Technology at the Hong Kong Polytechnic University. Currently, she holds the position of Research Assistant Professor in the same department. Her research interests focus on organic/organometallic materials and device engineering for sustanable energy development.

15214095, 0, Downloaded from https://advanced.onlinelibrary.wiley.com/doi/10.1002/adma.202501881 by HONG KONG POLYTECHNIC UNIVERSITY HU NG HOM, Wiley Online Library on [26.092025]. See the Terms



**Hongfang Liu** is currently a full professor of the School of Chemistry and Chemical Engineering, Huazhong University of Science and Technology. She received her Ph.D. from Huazhong University of Science and Technology in 2000. She worked in Hiroshima University as a foreign research professor in Venture Business Laboratory from 2003 to 2005 and she came to work at Huazhong University of Science and Technology in 2005. Her research interests mainly focus on material corrosion and service failure, functional materials design, and applications.



Wai-Yeung Wong (Raymond) obtained his B.Sc. (Hons.) and Ph.D. degrees from the University of Hong Kong. After postdoctoral work at Texas A&M University and the University of Cambridge, he joined Hong Kong Baptist University from 1998 to 2016 and he now works at the Hong Kong Polytechnic University as the Dean of the Faculty of Science and Chair Professor of Chemical Technology. His research focuses on organometallic and materials chemistry, especially aiming at developing multifunctional molecules and polymers. He was awarded the RSC Chemistry of the Transition Metals Award, FACS Distinguished Young Chemist Award, State Natural Science Award (Second-class) from China, and RGC Senior Research Fellowship, amongst others. He is a Fellow of the Royal Society of Chemistry and a Foreign Member of the European Academy of Sciences.